AIMS Mathematics, 7(9): 16067–16101.
DOI: 10.3934/math.2022880
Received: 02 April 2022
Revised: 08 June 2022
Accepted: 13 June 2022
Published: 30 June 2022

http://www.aimspress.com/journal/Math

Research article

Fuzzy fractional estimates of Swift-Hohenberg model obtained using the Atangana-Baleanu fractional derivative operator

Saima Rashid[1,*], Sobia Sultana[2], Bushra Kanwal[3], Fahd Jarad[4,5,6,*] and Aasma Khalid[7]

[1] Department of Mathematics, Government College University, Faisalabad, Pakistan
[2] Department of Mathematics, Imam Mohammad Ibn Saud Islamic University, Riyadh 12211, Saudi Arabia
[3] Department of Mathematical Sciences, Fatimah Jinnah Women's University, Rawalpindi, Pakistan
[4] Department of Mathematics, Çankaya University, Ankara, Türkiye
[5] Department of Medical Research, China Medical University Hospital, China Medical University, Taichung, Taiwan
[6] Department of Mathematics, King Abdulaziz University, Jeddah, Saudi Arabia
[7] Department of Mathematics, Government College Women's University, Faisalabad, Pakistan

* **Correspondence:** Email: saimarashid@gcuf.edu.pk, fahd@cankaya.edu.tr.

Abstract: Swift-Hohenberg equations are frequently used to model the biological, physical and chemical processes that lead to pattern generation, and they can realistically represent the findings. This study evaluates the Elzaki Adomian decomposition method (EADM), which integrates a semi-analytical approach using a novel hybridized fuzzy integral transform and the Adomian decomposition method. Moreover, we employ this strategy to address the fractional-order Swift-Hohenberg model (SHM) assuming g**H**-differentiability by utilizing different initial requirements. The Elzaki transform is used to illustrate certain characteristics of the fuzzy Atangana-Baleanu operator in the Caputo framework. Furthermore, we determined the generic framework and analytical solutions by successfully testing cases in the series form of the systems under consideration. Using the synthesized strategy, we construct the approximate outcomes of the SHM with visualizations of the initial value issues by incorporating the fuzzy factor $\varpi \in [0, 1]$ which encompasses the varying fractional values. Finally, the EADM is predicted to be effective and precise in generating the analytical results for dynamical fuzzy fractional partial differential equations that emerge in scientific disciplines.

Keywords: Elzaki transform; Atangana-Baleanu fractional derivative; Swift-Hohenberg equation; statistical inference
Mathematics Subject Classification: 46S40, 47H10, 54H25

1. Introduction

Fractional calculus (FC) is now universally recognized as a critical tool for describing real events [1–5]. While researchers regard FC as a valuable instrument in systematic inquiry, the presence of fractional formulations is treated in a variety of contexts [6, 7]. The dynamical characteristics of fractional differential equations systems are not only consistent with the current stage, but they generally supply an adequate explanation for previous phases [8, 9]. The conversion of integer-order Differential equation (DE)-regulated systems to fractional DE-regulated structures should be accurate due to the distinctiveness of the diversification process such that a simple modification might culminate in great variability in the output. In addition, the relatively new aspect postulated engages the generalized Mittag-Leffler function (MLF), which includes the core element, and the properties of this framework exasperate the completely new regimens to achieve numerous additional intriguing attributes that have been observed in significant contexts, including mean square deflection associations and broadening variability. Since its presentation in 2016 by Atangana and Baleanu [10], the novel fractional derivative operator has been successfully applied in a multitude of disciplines of research and development [11, 12]. In a swift manner, models applying the Atangana-Baleanu (AB) fractional derivative culminates in a stochastic process. The MLF has since been revealed to be a more powerful and critical filtration procedure than the index and exponential law, allowing the AB-fractional differentiation to be an appropriate computing tool for replicating progressively complex and crucial difficulties in the Caputo setting [13, 14]. Due to intrinsic non-orientation, these formulas are generally renowned for providing fractional DEs without any fabricated oddities, as in the instance of the Riemann-Liouville (RL) and Caputo derivatives [15–17]. We have also witnessed an increase in interest in numerical modelling among these operators. However, calculating these derivatives theoretically presents a slew of computational challenges (see [18–20]).

Partial differential equations (PDEs) have been progressively crucial in addressing systematic and engineering issues, such as electro-osmotic flow [21], heat flux [22], neural networks [23] and thermal energy [24]. Therefore, the indexing, parameters and parameter settings in PDEs could be unknown, or a fuzzy approximation of most of them will be revealed by tracking, exploration, competence or dependability breakdown, among other methods. As a consequence, instead of requiring high accuracy, characteristics and actual data, the avoidance of uncertainty frameworks can be leveraged to deal with vagueness and complexity. As a function of such ambiguity, generalized PDEs develop fuzzy PDEs. Due to the complexity in generating analytical models for imprecise PDEs in construction settings, a reliable and protracted computational approach for addressing ambiguous PDEs may be requested. Several studies targeting fractional PDEs and related applications in pattern generation, hypothesis, bifurcation, chaos, cryptography, advanced robotics, Markov chains, machine learning networks and management are included in the scheme of research. Few have been assessed and referred [25, 26] to obtain a comprehensive grasp of the structural factors.

Chang and Zadeh [27] first proposed the concept of fuzzy differentiability, which was then supported by Dubois and Prade [28], who formulated and applied the extension principle to this approach. Fuzzy set theory (FST) is a valuable tool for modeling unpredictable phenomena. As a result, fuzzy conceptions are often leveraged to describe a variety of natural phenomena. For specified real-life scenarios, fuzzy PDEs are an excellent means of modeling vagueness and misinterpretation in certain quantities, see [29–32]. Because of its relevance in a wide range of scientific disciplines, FST

has a profound correlation with FC [33]. Kandel and Byatt [34] proposed fuzzy DEs in 1978, while Agarwal et al. [35] were the first to investigate fuzziness and the RL differentiability concept by using the Hukuhara-differentiability notion. FST and FC both use a variety of computational methodologies to gain a better understanding of dynamic structures while reducing the unpredictability of their computation. Identifying precise analytical solutions in the case of FPDEs is a complicated process. Also, to demonstrate the competence and acceptability of the synthesized trajectory, experimental investigations incorporating parabolic PDEs were provided. According to Allahviranloo and Kermani [36], an explicit numerical solution to the fuzzy hyperbolic and parabolic equations is provided. The validity and resilience of the proposed system were investigated in order to demonstrate that it is inherently robust. Arqub et al. [37] expounded the fuzzy FDE by using the non-singular kernel in consideration of the differential formulation of the AB operator. Zhao et al. [38] contemplated the fuzzy-based strategy to suppress the massive outbreak of the novel coronavirus.

PDEs have been extensively exploited as a tool for evaluating a handful of particular configurations of impediments in order to determine their intrinsic influence. Among them are the effects on chaos, patterning determination, stochastic instability and malformation evolution. The Swift-Hohenberg model (SHM) has been employed to generate structures in relatively simple (Rayleig-Bénard convection) and complex materials and microbial organisms (for example-brain cells). Jack Swift and Pierre Hohenberg [39] examined a modified versionof the SHM:

$$\mathbf{D}_{\lambda}\tilde{\mathbf{U}} = \bar{s}\tilde{\mathbf{U}} - (1+\nabla^2)^2\tilde{\mathbf{U}} + \bar{N}(\tilde{\mathbf{U}}), \tag{1.1}$$

where $\tilde{\mathbf{U}}$ is scalar, $\bar{s}$ is a real constant and $\bar{N}(\tilde{\mathbf{U}})$ is a nonlinear component. The suggested approach has a wide range of applications in science, including in fields related to photonic lenses, electromagnetism, ecology, biochemistry, and liquid-crystal light-valve operations, see [40–42].

The goal of this study was to evaluate three distinct SHMs using a fuzzy fractional Atangana-Baleanu-Caputo (ABC) operator and the Elzaki Adomian decomposition method (EADM) described as follows:

$${}^{c}\mathbf{D}_{\lambda}^{\delta}\tilde{\mathbf{U}}(\mathbf{v},\lambda) + \frac{\partial^4}{\partial\mathbf{v}^4}\tilde{\mathbf{U}}(\mathbf{v},\lambda) + 2\frac{\partial^2}{\partial\mathbf{v}^2}\tilde{\mathbf{U}}(\mathbf{v},\lambda) + (1-\wp)\tilde{\mathbf{U}}(\mathbf{v},xi) + \tilde{\mathbf{U}}^3(\mathbf{v},\lambda) = 0,\ 0<\delta\le 1, \wp\in\mathbb{R}, \lambda>0. \tag{1.2}$$

The SHMfeaturing the diffusive component [43] is denoted as

$${}^{c}\mathbf{D}_{\lambda}^{\delta}\tilde{\mathbf{U}}(\mathbf{v},\lambda) + \frac{\partial^4}{\partial\mathbf{v}^4}\tilde{\mathbf{U}}(\mathbf{v},\lambda) + 2\frac{\partial^2}{\partial\mathbf{v}^2}\tilde{\mathbf{U}}(\mathbf{v},\lambda) - \eta\frac{\partial^3}{\partial\mathbf{v}^3}\tilde{\mathbf{U}}(\mathbf{v},\lambda) - \rho\tilde{\mathbf{U}}(\mathbf{v},\lambda) - 2\tilde{\mathbf{U}}^2(\mathbf{v},\lambda) + \tilde{\mathbf{U}}^3(\mathbf{v},\lambda) = 0, \tag{1.3}$$

where η and ρ are the diffusive and bifurcation real components, respectively.

The extended version of the SHM is described as follows:

$${}^{c}\mathbf{D}_{\lambda}^{\delta}\tilde{\mathbf{U}}(\mathbf{v},\lambda) + \frac{\partial^4}{\partial\mathbf{v}^4}\tilde{\mathbf{U}}(\mathbf{v},\lambda) + 2\frac{\partial^2}{\partial\mathbf{v}^2}\tilde{\mathbf{U}}(\mathbf{v},\lambda) + (1-\wp)\tilde{\mathbf{U}}(\mathbf{v},\lambda) = \tilde{\mathbf{U}}^p(\mathbf{v},\lambda) - \Big(\frac{\partial\tilde{\mathbf{U}}(\mathbf{v},\lambda)}{\partial\mathbf{v}}\Big)^p,\ p\ge 0. \tag{1.4}$$

Khan et al. [44] expounded the numerical findings of the SHM. In [45], Vishal et al. derived the analytical results configuring the initial conditions, $\tilde{\mathbf{U}}(\mathbf{v},0) = \frac{1}{10}\sin\left(\frac{\pi\mathbf{v}}{\varrho}\right)$. Moreover, the author of [46] examined a fractional order SHM that exhibits dispersion. Merdan recently applied the variational iteration method to achieve a closed form solution for the identical constraint as stated previously in [47]. The authors of [48] deployed the homotopy analysis method to achieve an analytical solution for the SHM.

Tarig Elzaki [49] proposed a remarkable development in 2001 to enable the system of analyzing ordinary DEs and PDEs in the temporal domain. This novel transformation is an improvement to earlier versions that really can assist in evaluating the numerical expression of PDEs by using a similar approach to the Laplace and Sumudu transformations.

The Adomian decomposition method (ADM) is an operational technique for dealing with functional equations that arise in engineering disciplines; it was first presented by Adomian [50]. The result is viewed as the summing of an infinite series, which eventually leads to the desired accuracy. This strategy is exact and inexpensive, so it does not necessitate the utilization of an irreducible matrix, compound integrals, or infinite series interpretations. There are no drawback scenarios identified for this technique. A lot of scholars have already used this methodology [51, 52].

Due to the aforementioned inclination, establishing the exact-approximate estimates of fuzzy fractional PDEs is a challenging task. The goal of this research was to create a trustworthy way of extracting estimated results for a fuzzy fractional SHM, that is, a generalized SHM with dispersion elements that are ambiguous in ICs due to the EADM, which models the development pattern under investigation. Because the EADM and the Elzaki transform are interconnected, the ADM is termed the fuzzy EADM. Using a new technique, the fractional-order SHM is studied. The effectiveness of the proposed framework is demonstrated by analyzing the accuracy of an identified research illustration. The outcomes containing an uncertainty element have been evaluated using contemporary strategies. The SHM was used to generate synthetic dynamic behavior. In a modelling experiment, we illustrate the utility and practicality of the offered approximate procedures for producing fuzzy algorithms. The proposed novel approach can address a huge spectrum of fuzzy fractional orders of nonlinear PDEs.

The remaining portion of the paper is organized as follows, Section 2 presents definitions and formulas for the fractional derivatives, the Elzaki transform and FST. Section 3 illustrates the computational procedure for the suggested EADM scheme. Section 4 is devoted to the implementation of the fuzzy EADM. Also, numerical simulations have been performed in consideration of an uncertainty parameter. At the end, Section 5 presents the epilogue.

2. Preliminaries

This part clearly explains certain key facts about the Elzaki transform, as well as several key factors related to the importance of FST and FC, see [53].

Definition 2.1. ([54,55]) We say that a mapping $\Xi : \mathbb{R} \mapsto [0, 1]$ will be a fuzzy number if the following assumptions holds true:
(1)Ξ is normal (for some $\mathbf{v}_0 \in \mathbb{R}; \Xi(\mathbf{v}_0) = 1$);
(2) Ξ is upper semi continuous;
(3) $\Xi(\mathbf{v}_1\lambda + (1-\lambda)\mathbf{v}_2) \geq (\Xi(\mathbf{v}_1) \wedge \Xi(\mathbf{v}_2)) \; \forall \lambda \in [0, 1], \; \mathbf{v}_1, \mathbf{v}_2 \in \mathbb{R}$, i.e Ξ is a convex fuzzy set;
(4) $cl\{\mathbf{v} \in \mathbb{R}, \Xi(\mathbf{v}) > 0\}$ is compact.

Definition 2.2. ([54]) A fuzzy number Ξ is said to be a ϖ-level set that can be stated as

$$[\Xi]^{\varpi} = \{\mathbf{U} \in \mathbb{R} : \Xi(\mathbf{U}) \geq \varpi\}, \tag{2.1}$$

where $\varpi \in [0, 1]$.

Definition 2.3. ([54]) We say that a fuzzy number has the parametric version $[\underline{\Xi}(\varpi), \bar{\Xi}(\varpi)]$ such that $\varpi \in [0,1]$ satisfies the subsequent assumptions:
(1) $\underline{\Xi}(\varpi)$ is non-decreasing, left continuous, bounded over $(0,1]$ and right continuous at 0.
(2) $\bar{\Xi}(\varpi)$ is non-increasing, left continuous, bounded over $(0,1]$ and right continuous at 0.
(3) $\underline{\Xi}(\varpi) \leq \bar{\Xi}(\varpi)$.
Also, Ξ is a crisp number (or singleton) if $\underline{\Xi}(\varpi) = \bar{\Xi}(\varpi)$ for every $\varpi \in [0,1]$.

Definition 2.4. ([53]) It is established that $\varpi \in [0,1]$ and Υ is a scalar. Assuming two fuzzy numbers $\tilde{\upsilon_1} = [\underline{\upsilon_1}, \bar{\upsilon_1}]$ *and* $\tilde{\upsilon_2} = [\underline{\upsilon_2}, \bar{\upsilon_2}]$, then the arithmetic characteristics are explained as follows:
(1) $\tilde{\upsilon_1} \oplus \tilde{\upsilon_2} = [\underline{\upsilon_1}(\varpi) \oplus \underline{\upsilon_2}(\varpi), \bar{\upsilon_1}(\varpi) \oplus \bar{\upsilon_2}(\varpi)]$;
(2) $\tilde{\upsilon_1} \ominus \tilde{\upsilon_2} = [\underline{\upsilon_1}(\varpi) \ominus \underline{\upsilon_2}(\varpi), \bar{\upsilon_1}(\varpi) \ominus \bar{\upsilon_2}(\varpi)]$;
(3) $\Upsilon \odot \tilde{\upsilon_1} = \begin{cases} [\Upsilon \odot \underline{\upsilon_1}, \Upsilon \odot \bar{\upsilon_1}] & \Upsilon \geq 0, \\ [\Upsilon \odot \bar{\upsilon_1}, \Upsilon \odot \underline{\upsilon_1}] & \Upsilon < 0. \end{cases}$

Definition 2.5. ([56]) Consider two fuzzy numbers $\tilde{\upsilon_1} = [\underline{\upsilon_1}, \bar{\upsilon_1}]$ *and* $\tilde{\upsilon_2} = [\underline{\upsilon_2}, \bar{\upsilon_2}]$; the Hausdorff distance d between fuzzy numbers is described as

$$d(\tilde{\upsilon_1}, \tilde{\upsilon_2}) = \sup_{\varpi \in [0,1]} [\max\{|\underline{\upsilon_1}(\varpi) - \underline{\upsilon_2}(\varpi)|, |\bar{\upsilon_1}(\varpi) - \bar{\upsilon_2}(\varpi)|\}]. \tag{2.2}$$

Specifically, $(\tilde{E}, d)$ is a metric space.

Definition 2.6. ([56]) Assume a fuzzy real-valued mapping $\Theta : \mathbb{R} \mapsto \tilde{E}$; if for any $\epsilon > 0$ $\exists\, \beta > 0$ and a constant factor of $\nu_0 \in \mathbb{R}$ such that we have

$$d(\Theta(\nu), \Theta(\nu_0)) < \epsilon; \quad whenever |\nu - \nu_0| < \beta, \tag{2.3}$$

then Θ is said to be continuous.

Definition 2.7. ([57]) Let $\beta_1, \beta_2 \in \tilde{E}$. The **H**-difference of β_1 and β_2 is the fuzzy number $\beta_3 = \beta_1 \ominus {}^{\mathbf{H}}\beta_2$ such that $\beta_1 = \beta_2 \oplus \beta_3$. Observe that $\beta_1 \ominus {}^{\mathbf{H}}\beta_2 \neq \beta_1 \ominus \beta_2$.

The $g\mathbf{H}$-difference β_3 of two fuzzy numbers $\beta_1, \beta_2 \in \mathbb{R}$ is defined as:

$$\beta_1 \ominus_{g\mathbf{H}} \beta_2 = \beta_3 \Leftrightarrow \begin{cases} (i) & \beta_1 = \beta_2 \oplus \beta_3 \\ or & \\ (ii) & \beta_2 = \beta_1 \oplus (-1)\beta_3, \end{cases}$$

The relationship between two cases is defined as

$$(\beta_1 \ominus_{g\mathbf{H}} \beta_2)_i[\varpi] := 0 \ominus_{\mathbf{H}} (-1)((\beta_1 \ominus_{g\mathbf{H}} \beta_2)_{ii}[\varpi]).$$

Definition 2.8. ([57]) The generalized Hukuhara derivative of a fuzzy-valued function $\Theta : (b_1, b_2) \to \tilde{E}$ at ζ_0 is defined as

$$\Theta'_{(i)-g\mathbf{H}}(\zeta_0) = \lim_{h \to 0} \frac{\Theta(\zeta_0 + h) \ominus_{\mathbf{H}} \Theta(\zeta_0)}{h},$$

if $(\Theta)'_{(i)-g\mathbf{H}}(\zeta_0) \in \tilde{E}$, we say that Θ is generalized Hukuhara differentiable ($g\mathbf{H}$-differentiable) at ζ_0.

Moreover, we say that Θ is $[(i)-g\mathbf{H}]$-differentiable at ζ_0 if

$$[\Theta'_{(i)-g\mathbf{H}}(\zeta_0)]^{\varpi} = \left[\left[\lim_{h\to 0}\frac{\underline{\Theta}(\zeta_0+h)\ominus_{\mathbf{H}}\underline{\Theta}(\zeta_0)}{h}\right]^{\varpi},\left[\lim_{h\to 0}\frac{\bar{\Theta}(\zeta_0+h)\ominus_{\mathbf{H}}\bar{\Theta}(\zeta_0)}{h}\right]^{\varpi}\right] = [(\underline{\Theta})'(\zeta_0,\varpi),(\bar{\Theta})'(\zeta_0,\varpi)], \tag{2.4}$$

and that Θ is $[(ii)-g\mathbf{H}]$-differentiable at ζ_0 if

$$\Theta'_{(ii)-g\mathbf{H}}(\zeta_0)=\lim_{h\to 0}\frac{\ominus_{\mathbf{H}}(-1)\Theta(\zeta_0+h)\oplus(-1)\Theta(\zeta_0)}{h}.$$

Also, we have

$$[\Theta'_{(ii)-g\mathbf{H}}(\zeta_0)]^{\varpi} = \left[\left[\lim_{h\to 0}\frac{\ominus_{\mathbf{H}}(-1)\bar{\Theta}(\zeta_0+h)\oplus(-1)\bar{\Theta}(\zeta_0)}{h}\right]^{\varpi},\left[\lim_{h\to 0}\frac{\ominus_{\mathbf{H}}(-1)\underline{\Theta}(\zeta_0+h)\oplus(-1)\underline{\Theta}(\zeta_0)}{h}\right]^{\varpi}\right] = [(\bar{\Theta})'(\zeta_0,\varpi),(\underline{\Theta})'(\zeta_0,\varpi)]. \tag{2.5}$$

Throughout this investigation, we symbolize Θ as (**1**)-differentiable and (**2**)-differentiable, respectively, if it is differentiable under the conditions described by Eqs (2.4) and (2.5) given by the aforementioned concept.

Theorem 2.1. *([53]) Assume a fuzzy-valued mapping* $\Theta : \mathbb{R}\mapsto\tilde{E}$ *such that* $\Theta(\zeta_0;\varpi)=[\underline{\Theta}(\zeta_0;\varpi),\bar{\Theta}(\zeta_0;\varpi)]$ *and* $\varpi\in[0,1]$. *Then*
I. $\underline{\Theta}(\zeta_0;\varpi)$ *and* $\bar{\Theta}(\zeta_0;\varpi)$ *are differentiable, if* Θ *is a* (***1***)*-differentiable, and*

$$[\Theta'(\zeta_0)]^{\varpi}=[\underline{\Theta}'(\zeta_0;\varpi),\bar{\Theta}'(\zeta_0;\varpi)]. \tag{2.6}$$

II. $\underline{\Theta}(\zeta_0;\varpi)$ *and* $\bar{\Theta}(\zeta_0;\varpi)$ *are differentiable, if* Θ *is a* (***2***)*-differentiable, and*

$$[\Theta'(\zeta_0)]^{\varpi}=[\bar{\Theta}'(\zeta_0;\varpi),\underline{\Theta}'(\zeta_0;\varpi)]. \tag{2.7}$$

Let $\mathbf{C}^F[a_1,b_1]$ be the space of all continuous fuzzy-valued functions on the interval $[a_1,b_1]$ and let there be a space of all Lebesgue integrable fuzzy-valued mapping $\mathcal{L}^F[a_1,b_1]$ on $[a_1,b_1]\subset\mathbb{R}$; then, the subsequent concept is presented follows:

Definition 2.9. ([52]) Consider a function $\mathbf{U}\in\mathbf{C}^F[a_1,b_1]\bigcap\mathcal{L}^F[a_1,b_1]$ represented in parameterized versions $\tilde{\mathbf{U}}=[\underline{\mathbf{U}}_{\varpi}(\lambda),\bar{\mathbf{U}}_{\varpi}(\lambda)]$, $\varpi\in[0,1]$ and $\lambda_0\in(a_1,b_1)$; then, the fuzzy fractional ABC operator is defined as

$${}^{ABC}\mathbf{D}^{\delta}_{g\mathbf{H}}\mathbf{U}(\lambda)=\frac{\mathbf{N}(\delta)}{(1-\delta)}\odot\int_0^{\lambda}E_{\delta}\Big(\frac{-\delta(\lambda-\mathbf{v})^{\delta}}{1-\delta}\Big)\odot\mathbf{U}'_{g\mathbf{H}}(\mathbf{v})d\mathbf{v}, \tag{2.8}$$

where $q=\lceil\varpi\rceil$ and

$$\mathbf{U}^{(q)}(\mathbf{v})=\lim_{\hbar\mapsto 0}\frac{\mathbf{U}^{(q-1)}(\mathbf{v}+\hbar)\ominus\,{}_{g\mathbf{H}}\mathbf{U}^{(q-1)}(\mathbf{v})}{\hbar}.$$

The $g\mathbf{H}$-difference is stated in two ways:
• $(i) - g\mathbf{H}$ differentiable:

$$\mathbf{U}^{(q)}_{(i)-g\mathbf{H}}(\mathbf{v}) = \lim_{\hbar \mapsto 0} \frac{\mathbf{U}^{(q-1)}(\mathbf{v}+\hbar) \ominus {}_{\mathbf{H}}\mathbf{U}^{(q-1)}(\mathbf{v})}{\hbar}. \tag{2.9}$$

$$^{ABC}\mathbf{D}^{\delta}_{(i)-g\mathbf{H}}\mathbf{U}(\lambda_0;\varpi) = \Big[{}^{ABC}\mathbf{D}^{\delta}_{(i)-g\mathbf{H}}\underline{\mathbf{U}}(\lambda_0;\varpi),\ {}^{ABC}\mathbf{D}^{\delta}_{(i)-g\mathbf{H}}\bar{\mathbf{U}}(\lambda_0;\varpi)\Big].$$

• $(ii) - g\mathbf{H}$ differentiable:

$$\mathbf{U}^{(q)}_{(ii)-g\mathbf{H}}(\mathbf{v}) = \lim_{\hbar \mapsto 0} \frac{\mathbf{U}^{(q-1)}(\mathbf{v}) \ominus {}_{\mathbf{H}}\mathbf{U}^{(q-1)}(\mathbf{v}+\hbar)}{\hbar}. \tag{2.10}$$

$$^{ABC}\mathbf{D}^{\delta}_{(ii)-g\mathbf{H}}\mathbf{U}(\lambda_0;\varpi) = \Big[{}^{ABC}\mathbf{D}^{\delta}_{(ii)-g\mathbf{H}}\bar{\mathbf{U}}(\lambda_0;\varpi),\ {}^{ABC}\mathbf{D}^{\delta}_{(ii)-g\mathbf{H}}\underline{\mathbf{U}}(\lambda_0;\varpi)\Big].$$

Both of these are stated as the following formulation for $q-1 < \delta < q$:

$$\begin{aligned}
^{ABC}\mathbf{D}^{\delta}_{(i)-g\mathbf{H}}\underline{\mathbf{U}}(\lambda;\varpi) &= \frac{\mathbf{N}(\delta)}{1-\delta}\Big[\int_0^{\lambda} \underline{\mathbf{U}}'_{(i)-g\mathbf{H}}(\mathbf{v})E_{\delta}\Big(\frac{-\delta(\lambda-\mathbf{v})^{\delta}}{1-\delta}\Big)d\mathbf{v}\Big]_{\lambda=\lambda_0},\\
^{ABC}\mathbf{D}^{\delta}_{(i)-g\mathbf{H}}\bar{\mathbf{U}}(\lambda;\varpi) &= \frac{\mathbf{N}(\delta)}{1-\delta}\Big[\int_0^{\lambda} \bar{\mathbf{U}}'_{(i)-g\mathbf{H}}(\mathbf{v})E_{\delta}\Big(\frac{-\delta(\lambda-\mathbf{v})^{\delta}}{1-\delta}\Big)d\mathbf{v}\Big]_{\lambda=\lambda_0}.
\end{aligned} \tag{2.11}$$

Definition 2.10. ([49]) Suppose there is a continuous fuzzy function $\mathbf{U}$ and a collection $\mathcal{M}$ with an exponential function described as

$$\mathcal{M} = \Big\{\mathbf{U}(\lambda) : \exists z, p_1, p_2 > 0, \big|\mathbf{U}(\lambda)\big| < ze^{\frac{|\lambda|}{p_i}},\ if\ \lambda \in (-1)^i \times [0,\infty)|\Big\}, \tag{2.12}$$

where z is assumed to be finite, but p_1 *and* p_2 may be finite or infinite; therefore, the fuzzy Elzaki transform (FET) is described as

$$\mathbb{E}\{\tilde{\mathbf{U}}(\lambda)\}(\varphi) = \mathbf{Q}(\varphi) = \varphi\int_0^{\infty} e^{-\frac{\lambda}{\varphi}} \odot \tilde{\mathbf{U}}(\lambda)d\lambda, \quad \lambda \geq 0,\ \ \varphi \in [p_1, p_2]. \tag{2.13}$$

The prescribed parametric expression of $\tilde{\mathbf{U}}(\lambda)$ is defined as

$$\varphi\int_0^{\infty} e^{-\frac{\lambda}{\varphi}}\tilde{\mathbf{U}}(\lambda)d\lambda = \Big[\varphi\int_0^{\infty} e^{-\frac{\lambda}{\varphi}}\underline{\mathbf{U}}(\lambda)d\lambda, \varphi\int_0^{\infty} e^{-\frac{\lambda}{\varphi}}\bar{\mathbf{U}}(\lambda)d\lambda\Big]. \tag{2.14}$$

Thus,

$$\mathbb{E}[\mathbf{U}(\lambda,\varpi)] = [\underline{\mathbf{E}}(\lambda,\varpi), \bar{\mathbf{E}}(\lambda,\varpi)]. \tag{2.15}$$

Yuvaz and Abdeljawad [58] proposed the ABC operator form of the Elzaki transform. Following this tendency, the fuzzified version of the ABC-fractional derivative associated with the Elzaki transform will be described as follows,

Definition 2.11. ([52]) For $\delta \in (0,1]$, surmise that $\mathbf{U} \in \mathbf{C}^F[0,\bar{d}_1] \bigcap \mathcal{L}^F[0,\bar{d}_1]$ such that $\tilde{\mathbf{U}}(\lambda) = [\underline{\mathbf{U}}(\lambda,\varpi), \bar{\mathbf{U}}(\lambda,\varpi)]$, $\varpi \in [0,1]$; then, the Elzaki transform of the ABC-$g\mathbf{H}$ operator is defined as

$$\mathbb{E}\Big[{}^{ABC}\mathbf{D}^{\delta}_{g\mathbf{H}}\tilde{\mathbf{U}}(\lambda)\Big] = \varphi \int_0^{\infty} e^{-\frac{\lambda}{\varphi}} \odot {}^{ABC}\mathbf{D}^{\delta}_{g\mathbf{H}}\mathbf{U}(\lambda)d\lambda$$

and

$$\begin{aligned}\mathbb{E}\Big[{}^{ABC}\mathbf{D}^{\delta}_{g\mathbf{H}}\tilde{\mathbf{U}}(\lambda;\varpi)\Big] &= \Big[\mathbb{E}\Big[{}^{ABC}\mathbf{D}^{\delta}_{g\mathbf{H}}\underline{\mathbf{U}}(\lambda;\varpi)\Big], \mathbb{E}\Big[{}^{ABC}\mathbf{D}^{\delta}_{g\mathbf{H}}\bar{\mathbf{U}}(\lambda;\varpi)\Big]\Big]\\ &= \varphi \int_0^{\infty} e^{-\frac{\lambda}{\varphi}}\Big[{}^{ABC}\mathbf{D}^{\delta}_{g\mathbf{H}}\underline{\mathbf{U}}(\lambda;\varpi),\ {}^{ABC}\mathbf{D}^{\delta}_{g\mathbf{H}}\bar{\mathbf{U}}(\lambda;\varpi)\Big]d\lambda\\ &= \Big[\varphi \int_0^{\infty} e^{-\frac{\lambda}{\varphi}}\,{}^{ABC}\mathbf{D}^{\delta}_{g\mathbf{H}}\underline{\mathbf{U}}(\lambda;\varpi)d\lambda, \varphi \int_0^{\infty} e^{-\frac{\lambda}{\varphi}}\,{}^{ABC}\mathbf{D}^{\delta}_{g\mathbf{H}}\bar{\mathbf{U}}(\lambda;\varpi)d\lambda\Big].\end{aligned}$$

Thus, we have

$$\begin{aligned}\mathbb{E}\Big[{}^{ABC}\mathbf{D}^{\delta}_{g\mathbf{H}}\underline{\mathbf{U}}(\lambda;\varpi)\Big] &= \varphi \int_0^{\infty} e^{-\frac{\lambda}{\varphi}}\,{}^{ABC}\mathbf{D}^{\delta}_{g\mathbf{H}}\underline{\mathbf{U}}(\lambda;\varpi)d\lambda,\\ \mathbb{E}\Big[{}^{ABC}\mathbf{D}^{\delta}_{g\mathbf{H}}\bar{\mathbf{U}}(\lambda;\varpi)\Big] &= \varphi \int_0^{\infty} e^{-\frac{\lambda}{\varphi}}\,{}^{ABC}\mathbf{D}^{\delta}_{g\mathbf{H}}\bar{\mathbf{U}}(\lambda;\varpi)d\lambda.\end{aligned} \tag{2.16}$$

• $(i) - g\mathbf{H}$ differentiability:

$$\begin{aligned}{}^{ABC}\mathbf{D}^{\delta}_{(i)-g\mathbf{H}}\mathbf{U}(\mathbf{v};\varpi) &= \Big[{}^{ABC}\mathbf{D}^{\delta}\underline{Q}(\mathbf{v};\varpi),\ {}^{ABC}\mathbf{D}^{\delta}\bar{Q}(\mathbf{v};\varpi)\Big],\\ \mathbb{E}\Big({}^{ABC}\mathbf{D}^{\delta}_{(i)-g\mathbf{H}}\mathbf{U}(\mathbf{v};\varpi)\Big) &= \frac{\mathbf{N}(\delta)}{\delta\varphi^{\delta}+1-\delta} \odot \frac{\mathbf{E}[\mathbf{U}(\lambda,\varpi)]}{\varphi} \ominus \varphi^2 \odot \frac{\mathbf{N}(\delta)}{\delta\varphi^{\delta}+1-\delta} \odot \mathbf{U}(0).\end{aligned} \tag{2.17}$$

• $(ii) - g\mathbf{H}$ differentiability:

$$\begin{aligned}{}^{ABC}\mathbf{D}^{\delta}_{(ii)-g\mathbf{H}}\mathbf{U}(\mathbf{v};\varpi) &= \Big[{}^{ABC}\mathbf{D}^{\delta}\bar{Q}(\mathbf{v};\varpi),\ {}^{ABC}\mathbf{D}^{\delta}\underline{Q}(\mathbf{v};\varpi)\Big],\\ \mathbb{E}\Big({}^{ABC}\mathbf{D}^{\delta}_{(ii)-g\mathbf{H}}\mathbf{U}(\mathbf{v};\varpi)\Big) &= (-1)\varphi^2 \odot \frac{\mathbf{N}(\delta)}{\delta\varphi^{\delta}+1-\delta} \odot \mathbf{U}(0) \ominus {}_{\mathbf{H}}(-1)\frac{\mathbf{N}(\delta)}{\delta\varphi^{\delta}+1-\delta} \odot \frac{\mathbf{E}[\mathbf{U}(\lambda,\varpi)]}{\varphi}.\end{aligned} \tag{2.18}$$

3. Road map for proposed strategy

The underlying process for generating the estimated findings of a fractional-order SHM employing the fuzzy fractional ABC operator in the FET is described and evaluated.

The following descriptive framework of (1.1) is as follows:

$$\begin{cases} \frac{\partial^{\delta}}{\partial\lambda^{\delta}}\underline{\mathbf{U}}(\mathbf{v},\lambda;\varpi) = (\wp-1)\underline{\mathbf{U}}(\mathbf{v},\lambda;\varpi) - \frac{\partial^4}{\partial\mathbf{v}^4}\underline{\mathbf{U}}(\mathbf{v},\lambda;\varpi) - 2\frac{\partial^2}{\partial\mathbf{v}^2}\underline{\mathbf{U}}(\mathbf{v},\lambda;\varpi) - \underline{\mathbf{U}}^3(\mathbf{v},\lambda;\varpi), \\ \underline{\mathbf{U}}(\mathbf{v},0) = \underline{Q}(\mathbf{v};\varpi), \\ \frac{\partial^{\delta}}{\partial\lambda^{\delta}}\bar{\mathbf{U}}(\mathbf{v},\lambda;\varpi) = (\wp-1)\bar{\mathbf{U}}(\mathbf{v},\lambda;\varpi) - \frac{\partial^4}{\partial\mathbf{v}^4}\bar{\mathbf{U}}(\mathbf{v},\lambda;\varpi) - 2\frac{\partial^2}{\partial\mathbf{v}^2}\bar{\mathbf{U}}(\mathbf{v},\lambda;\varpi) - \bar{\mathbf{U}}^3(\mathbf{v},\lambda;\varpi), \\ \bar{\mathbf{U}}(\mathbf{v},0) = \bar{Q}(\mathbf{v};\varpi). \end{cases} \tag{3.1}$$

Applying the FET to the first case in Eq (3.1), we have

$$\mathbb{E}[\underline{\mathbf{U}}(\mathbf{v},\lambda;\varpi)] = \mathbb{E}\Big[(\wp-1)\underline{\mathbf{U}}(\mathbf{v},\lambda;\varpi) - \frac{\partial^4}{\partial\mathbf{v}^4}\underline{\mathbf{U}}(\mathbf{v},\lambda;\varpi) - 2\frac{\partial^2}{\partial\mathbf{v}^2}\underline{\mathbf{U}}(\mathbf{v},\lambda;\varpi) - \underline{\mathbf{U}}^3(\mathbf{v},\lambda;\varpi)\Big].$$

Given the IC $\underline{\mathbf{U}}(\mathbf{v},0) = \underline{Q}(\mathbf{v})$, we have

$$\begin{aligned} &\frac{\mathbf{N}(\delta)}{1-\delta+\delta\varphi^{\delta}}\mathbb{E}[\underline{\mathbf{U}}(\mathbf{v},\lambda;\varpi)] - \frac{\varphi^2\mathbf{N}(\delta)}{1-\delta+\delta\varphi^{\delta}}\underline{\mathbf{U}}_{(\kappa)}(\mathbf{v};\varpi) \\ &= \mathbb{E}\Big[(\wp-1)\underline{\mathbf{U}}(\mathbf{v},\lambda;\varpi) - \frac{\partial^4}{\partial\mathbf{v}^4}\underline{\mathbf{U}}(\mathbf{v},\lambda;\varpi) - 2\frac{\partial^2}{\partial\mathbf{v}^2}\underline{\mathbf{U}}(\mathbf{v},\lambda;\varpi) - \underline{\mathbf{U}}^3(\mathbf{v},\lambda;\varpi)\Big]. \end{aligned}$$

Alternatively, we get

$$\begin{aligned} \mathbb{E}[\underline{\mathbf{U}}(\mathbf{v},\lambda;\varpi)] \quad &= \varphi^2\underline{Q}(\mathbf{v};\varpi) \\ &+\frac{1-\delta+\delta\varphi^{\delta}}{\mathbf{N}(\delta)}\mathbb{E}\Big[(\wp-1)\underline{\mathbf{U}}(\mathbf{v},\lambda;\varpi) - \frac{\partial^4}{\partial\mathbf{v}^4}\underline{\mathbf{U}}(\mathbf{v},\lambda;\varpi) - 2\frac{\partial^2}{\partial\mathbf{v}^2}\underline{\mathbf{U}}(\mathbf{v},\lambda;\varpi) \\ &-\underline{\mathbf{U}}^3(\mathbf{v},\lambda;\varpi)\Big]. \end{aligned} \tag{3.2}$$

The result for the undetermined series is defined as

$$\underline{\mathbf{U}}(\mathbf{v},\lambda;\varpi) = \sum_{q=0}^{\infty}\underline{\mathbf{U}}(\mathbf{v},\lambda;\varpi). \tag{3.3}$$

Ultimately, the nonlinear factors are discarded as

$$\underline{\mathcal{N}}(\mathbf{v},\lambda;\varpi) = \sum_{q=0}^{\infty}\underline{\mathbf{A}}_q(\mathbf{v},\lambda;\varpi), \tag{3.4}$$

where $\underline{\mathbf{A}}_q$ is expressed in the form of an Adomian polynomial, which is defined as

$$\underline{\mathbf{A}}_q = \frac{1}{q!}\frac{d^q}{d\rho^q}\Big[\underline{\mathcal{N}}\Big(\sum_{q=0}^{\infty}\rho^q\underline{\mathbf{U}}_q(\mathbf{v},\lambda;\varpi)\Big)\Big]_{\rho=0}. \tag{3.5}$$

Further, Eq (3.2) can be specified as

$$\mathbb{E}\Big[\sum_{q=0}^{\infty}\underline{\mathbf{U}}(\mathbf{v},\lambda;\varpi)\Big] \quad = \varphi^2\underline{Q}(\mathbf{v};\varpi) + \frac{1-\delta+\delta\varphi^{\delta}}{\mathbf{N}(\delta)}$$

$$\times\mathbb{E}\Big[(\wp-1)\sum_{q=0}^{\infty}\underline{\mathbf{U}}(\mathbf{v},\lambda;\varpi)-\frac{\partial^4}{\partial\mathbf{v}^4}\sum_{q=0}^{\infty}\underline{\mathbf{U}}(\mathbf{v},\lambda;\varpi)-2\frac{\partial^2}{\partial\mathbf{v}^2}\sum_{q=0}^{\infty}\underline{\mathbf{U}}(\mathbf{v},\lambda;\varpi)$$
$$-\sum_{q=0}^{\infty}\underline{\mathbf{A}}(\mathbf{v},\lambda;\varpi)\Big]. \tag{3.6}$$

In view of the inverse FET, we attain

$$\begin{aligned}
\underline{\mathbf{U}}_0(\mathbf{v},\lambda;\varpi) &= \mathbb{E}^{-1}\Big[\varphi^2\underline{Q}(\mathbf{v};\varpi)\Big],\\
\underline{\mathbf{U}}_1(\mathbf{v},\lambda;\varpi) &= \mathbb{E}^{-1}\Big[\frac{1-\delta+\delta\varphi^{\delta}}{\mathbf{N}(\delta)}\mathbb{E}\Big[(\wp-1)\underline{\mathbf{U}}_0(\mathbf{v},\lambda;\varpi)-\frac{\partial^4}{\partial\mathbf{v}^4}\underline{\mathbf{U}}_0(\mathbf{v},\lambda;\varpi)-2\frac{\partial^2}{\partial\mathbf{v}^2}\underline{\mathbf{U}}_0(\mathbf{v},\lambda;\varpi)\\
&\quad -\underline{\mathbf{A}}_0(\mathbf{v},\lambda;\varpi)\Big]\Big],\\
\underline{\mathbf{U}}_2(\mathbf{v},\lambda;\varpi) &= \mathbb{E}^{-1}\Big[\frac{1-\delta+\delta\varphi^{\delta}}{\mathbf{N}(\delta)}\mathbb{E}\Big[(\wp-1)\underline{\mathbf{U}}_1(\mathbf{v},\lambda;\varpi)-\frac{\partial^4}{\partial\mathbf{v}^4}\underline{\mathbf{U}}_1(\mathbf{v},\lambda;\varpi)-2\frac{\partial^2}{\partial\mathbf{v}^2}\underline{\mathbf{U}}_1(\mathbf{v},\lambda;\varpi)\\
&\quad -\underline{\mathbf{A}}_1(\mathbf{v},\lambda;\varpi)\Big]\Big],\\
&\vdots\\
\underline{\mathbf{U}}_{q+1}(\mathbf{v},\lambda;\varpi) &= \mathbb{E}^{-1}\Big[\frac{1-\delta+\delta\varphi^{\delta}}{\mathbf{N}(\delta)}\mathbb{E}\Big[(\wp-1)\underline{\mathbf{U}}_q(\mathbf{v},\lambda;\varpi)-\frac{\partial^4}{\partial\mathbf{v}^4}\underline{\mathbf{U}}_q(\mathbf{v},\lambda;\varpi)-2\frac{\partial^2}{\partial\mathbf{v}^2}\underline{\mathbf{U}}_q(\mathbf{v},\lambda;\varpi)\\
&\quad -\underline{\mathbf{A}}_q(\mathbf{v},\lambda;\varpi)\Big]\Big].
\end{aligned} \tag{3.7}$$

$$\underline{\mathbf{U}}(\mathbf{v},\lambda;\varpi)=\underline{\mathbf{U}}_0(\mathbf{v},\lambda;\varpi)+\underline{\mathbf{U}}_1(\mathbf{v},\lambda;\varpi)+\dots. \tag{3.8}$$

As a result, the upper version of Eq (3.1) is viewed in the identical manner. Furthermore, we provide the solution's parameterized version, which is characterized as follows:

$$\begin{cases}\underline{\mathbf{U}}(\mathbf{v},\lambda;\varpi)=\underline{\mathbf{U}}_0(\mathbf{v},\lambda;\varpi)+\underline{\mathbf{U}}_1(\mathbf{v},\lambda;\varpi)+\dots,\\ \bar{\mathbf{U}}(\mathbf{v},\lambda;\varpi)=\bar{\mathbf{U}}_0(\mathbf{v},\lambda;\varpi)+\bar{\mathbf{U}}_1(\mathbf{v},\lambda;\varpi)+\dots.\end{cases} \tag{3.9}$$

4. Mathematical analysis of analytical results

In the following sections, we will employ the EADM to determine the approximate findings for the SHMusing the fuzzy fractionalABC operatorunder various initial assumptions.

To commence, we evaluate the SHM given by Eq (1.1) consideringthe EADM.

Example 4.1. Suppose that the fuzzy fractional-order SHM has fuzzy ICs

$$\begin{aligned}
&\frac{\partial^{\delta}}{\partial\lambda^{\delta}}\tilde{\mathbf{U}}(\mathbf{v},\lambda;\varpi)=(\wp-1)\odot\tilde{\mathbf{U}}(\mathbf{v},\lambda;\varpi)\ominus\frac{\partial^4}{\partial\mathbf{v}^4}\tilde{\mathbf{U}}(\mathbf{v},\lambda;\varpi)\ominus 2\odot\frac{\partial^2}{\partial\mathbf{v}^2}\tilde{\mathbf{U}}(\mathbf{v},\lambda;\varpi)-\tilde{\mathbf{U}}^3(\mathbf{v},\lambda;\varpi),\\
&\tilde{\mathbf{U}}(\mathbf{v},0)=\tilde{\Upsilon}(\varpi)\odot\exp(\mathbf{v}),
\end{aligned} \tag{4.1}$$

where $\tilde{\Upsilon}(\varpi)=[\underline{\Upsilon}(\varpi),\bar{\Upsilon}(\varpi)]=[\varpi-1,1-\varpi]$ and there is a fuzzy number $\varpi\in[0,1]$.

The parametric form of Eq (4.1) presents as:

$$\begin{cases} \frac{\partial^{\delta}}{\partial\lambda^{\delta}}\underline{\mathbf{U}}(\mathbf{v},\lambda;\varpi) = (\wp-1)\underline{\mathbf{U}}(\mathbf{v},\lambda;\varpi) - \frac{\partial^4}{\partial\mathbf{v}^4}\underline{\mathbf{U}}(\mathbf{v},\lambda;\varpi) - 2\frac{\partial^2}{\partial\mathbf{v}^2}\underline{\mathbf{U}}(\mathbf{v},\lambda;\varpi) - \underline{\mathbf{U}}^3(\mathbf{v},\lambda;\varpi), \\ \underline{\mathbf{U}}(\mathbf{v},0) = \underline{\Upsilon}(\varpi)\exp(\mathbf{v}), \\ \frac{\partial^{\delta}}{\partial\lambda^{\delta}}\bar{\mathbf{U}}(\mathbf{v},\lambda;\varpi) = (\wp-1)\bar{\mathbf{U}}(\mathbf{v},\lambda;\varpi) - \frac{\partial^4}{\partial\mathbf{v}^4}\bar{\mathbf{U}}(\mathbf{v},\lambda;\varpi) - 2\frac{\partial^2}{\partial\mathbf{v}^2}\bar{\mathbf{U}}(\mathbf{v},\lambda;\varpi) - \bar{\mathbf{U}}^3(\mathbf{v},\lambda;\varpi), \\ \bar{\mathbf{U}}(\mathbf{v},0) = \bar{\Upsilon}(\varpi)\exp(\mathbf{v}). \end{cases} \tag{4.2}$$

We examine the first instance of Eq (4.2) in an attempt to determine the EADM solution. In view of the procedure outlined in Section 3, we have

$$\begin{aligned} &\frac{\mathbf{N}(\delta)}{1-\delta+\delta\varphi^{\delta}}\mathbb{E}[\underline{\mathbf{U}}(\mathbf{v},\lambda;\varpi)] - \frac{\varphi^2\mathbf{N}(\delta)}{1-\delta+\delta\varphi^{\delta}}\underline{\mathbf{U}}_{(\kappa)}(\mathbf{v};\varpi) \\ &= \mathbb{E}\Big[(\wp-1)\underline{\mathbf{U}}(\mathbf{v},\lambda;\varpi) - \frac{\partial^4}{\partial\mathbf{v}^4}\underline{\mathbf{U}}(\mathbf{v},\lambda;\varpi) - 2\frac{\partial^2}{\partial\mathbf{v}^2}\underline{\mathbf{U}}(\mathbf{v},\lambda;\varpi) - \underline{\mathbf{U}}^3(\mathbf{v},\lambda;\varpi)\Big]. \end{aligned}$$

Simple calculations yield

$$\begin{aligned} \underline{\mathbf{U}}(\mathbf{v},\lambda;\varpi) \quad &= (\varpi-1)\exp(\mathbf{v}) + \mathbb{E}^{-1}\Bigg[\frac{1-\delta+\delta\varphi^{\delta}}{\mathbf{N}(\delta)} \\ &\times\mathbb{E}\Big[(\wp-1)\underline{\mathbf{U}}(\mathbf{v},\lambda;\varpi) - \frac{\partial^4}{\partial\mathbf{v}^4}\underline{\mathbf{U}}(\mathbf{v},\lambda;\varpi) - 2\frac{\partial^2}{\partial\mathbf{v}^2}\underline{\mathbf{U}}(\mathbf{v},\lambda;\varpi) - \underline{\mathbf{U}}^3(\mathbf{v},\lambda;\varpi)\Big]\Bigg]. \end{aligned} \tag{4.3}$$

We assume the infinite sum $\underline{\mathbf{U}}(\mathbf{v},\lambda;\varpi) = \sum_{q=0}^{\infty}\underline{\mathbf{U}}_q(\mathbf{v},\lambda;\varpi)$ incorporates Eq (3.5) and validates the non-linearity. As a result, Eq (4.3) leads to the formation

$$\begin{aligned} \sum_{q=0}^{\infty}\underline{\mathbf{U}}_q(\mathbf{v},\lambda;\varpi) \quad &= (\varpi-1)\exp(\mathbf{v}) + \mathbb{E}^{-1}\Bigg[\frac{1-\delta+\delta\varphi^{\delta}}{\mathbf{N}(\delta)} \\ &\times\mathbb{E}\Big[(\wp-1)\sum_{q=0}^{\infty}\underline{\mathbf{U}}_q(\mathbf{v},\lambda;\varpi) - \frac{\partial^4}{\partial\mathbf{v}^4}\sum_{q=0}^{\infty}\underline{\mathbf{U}}_q(\mathbf{v},\lambda;\varpi) - 2\frac{\partial^2}{\partial\mathbf{v}^2}\sum_{q=0}^{\infty}\underline{\mathbf{U}}_q(\mathbf{v},\lambda;\varpi) \\ &- \sum_{q=0}^{\infty}\underline{\mathbf{A}}_q(\mathbf{v},\lambda;\varpi)\Big]\Bigg]. \end{aligned} \tag{4.4}$$

By virtue of Eq (3.4), we obtain

$$\underline{\mathbf{A}}_q(\underline{\mathbf{U}}^3) = \begin{cases} \underline{\mathbf{U}}_0^3, & q=0 \\ 3\underline{\mathbf{U}}_0^2\underline{\mathbf{U}}_1, & q=1 \\ 3\underline{\mathbf{U}}_0^2\underline{\mathbf{U}}_1^2 + 3\underline{\mathbf{U}}_0^2\underline{\mathbf{U}}_2, & q=2 \\ \underline{\mathbf{U}}_1^3 + 4\underline{\mathbf{U}}_0\underline{\mathbf{U}}_2 + 2\underline{\mathbf{U}}_0\underline{\mathbf{U}}_1\underline{\mathbf{U}}_2 + 3\underline{\mathbf{U}}_0\underline{\mathbf{U}}_3 & q=3. \end{cases} \tag{4.5}$$

Then, Eq (4.4) diminishes to

$$\underline{\mathbf{U}}_0(\mathbf{v},\lambda;\varpi) \quad = (\varpi-1)\exp(\mathbf{v}),$$

$$
\begin{aligned}
\underline{\underline{\mathbf{U}_1}}(\mathbf{v},\lambda;\varpi) &= \mathbb{E}^{-1}\Big[\frac{1-\delta+\delta\varphi^{\delta}}{\mathbf{N}(\delta)}\mathbb{E}\Big[(\wp-1)\underline{\mathbf{U}}_0(\mathbf{v},\lambda;\varpi)-\frac{\partial^4}{\partial\mathbf{v}^4}\underline{\mathbf{U}}_0(\mathbf{v},\lambda;\varpi)-2\frac{\partial^2}{\partial\mathbf{v}^2}\underline{\mathbf{U}}_0(\mathbf{v},\lambda;\varpi)\\
&\quad -\underline{\mathbf{A}}_0(\mathbf{v},\lambda;\varpi)\Big]\Big]\\
&= \frac{(\varpi-1)(\wp-4)\exp(\mathbf{v})-(\varpi-1)^3\exp(3\mathbf{v})}{\mathbf{N}(\delta)}\Big\{\frac{\delta\lambda^{\delta}}{\Gamma(\delta+1)}+(1-\delta)\Big\},\\
\underline{\underline{\mathbf{U}_2}}(\mathbf{v},\lambda;\varpi) &= \mathbb{E}^{-1}\Big[\frac{1-\delta+\delta\varphi^{\delta}}{\mathbf{N}(\delta)}\mathbb{E}\Big[(\wp-1)\underline{\mathbf{U}}_1(\mathbf{v},\lambda;\varpi)-\frac{\partial^4}{\partial\mathbf{v}^4}\underline{\mathbf{U}}_1(\mathbf{v},\lambda;\varpi)-2\frac{\partial^2}{\partial\mathbf{v}^2}\underline{\mathbf{U}}_1(\mathbf{v},\lambda;\varpi)\\
&\quad -\underline{\mathbf{A}}_1(\mathbf{v},\lambda;\varpi)\Big]\Big]\\
&= \frac{(\varpi-1)(\wp-4)^2\exp(\mathbf{v})-(112-4\wp)(\varpi-1)^3\exp(3\mathbf{v})+30(\varpi-1)^5\exp(5\mathbf{v})}{\mathbf{N}^2(\delta)}\\
&\quad \times\Big\{\frac{\delta^2\lambda^{2\delta}}{\Gamma(2\delta+1)}+2\delta(1-\delta)\frac{\lambda^{\delta}}{\Gamma(\delta+1)}+(1-\delta)^2\Big\},\\
&\quad \vdots .
\end{aligned}
$$

In a similar way, the further elements of the EADM system $\underline{\mathbf{U}}q$ ($q \geq 3$) can be identified. Furthermore, as the iterative technique develops, the attained result's trustworthiness improves significantly, and the established result appears progressively comparable to the expressive context. As a result, we have formulated a set of solutions that are structured in a series of formulations; that is,

$$\tilde{\mathbf{U}}(\mathbf{v},\lambda,\varpi) = \tilde{\mathbf{U}}_0(\mathbf{v},\lambda,\varpi)+\tilde{\mathbf{U}}_1(\mathbf{v},\lambda,\varpi)+\tilde{\mathbf{U}}_1(\mathbf{v},\lambda,\varpi)+\ldots$$

such that

$$
\begin{aligned}
\underline{\mathbf{U}}(\mathbf{v},\lambda,\varpi) &= \underline{\mathbf{U}}_0(\mathbf{v},\lambda,\varpi)+\underline{\mathbf{U}}_1(\mathbf{v},\lambda,\varpi)+\underline{\mathbf{U}}_1(\mathbf{v},\lambda,\varpi)+\ldots,\\
\bar{\mathbf{U}}(\mathbf{v},\lambda,\varpi) &= \bar{\mathbf{U}}_0(\mathbf{v},\lambda,\varpi)+\bar{\mathbf{U}}_1(\mathbf{v},\lambda,\varpi)+\bar{\mathbf{U}}_1(\mathbf{v},\lambda,\varpi)+\ldots.
\end{aligned}
$$

Eventually, we get

$$
\begin{aligned}
&\underline{\mathbf{U}}(\mathbf{v},\lambda,\varpi)\\
&= (\varpi-1)\exp(\mathbf{v})+\frac{(\varpi-1)(\wp-4)\exp(\mathbf{v})-(\varpi-1)^3\exp(3\mathbf{v})}{\mathbf{N}(\delta)}\Big\{\frac{\delta\lambda^{\delta}}{\Gamma(\delta+1)}+(1-\delta)\Big\}\\
&\quad +\frac{(\varpi-1)(\wp-4)^2\exp(\mathbf{v})-(112-4\wp)(\varpi-1)^3\exp(3\mathbf{v})+30(\varpi-1)^5\exp(5\mathbf{v})}{\mathbf{N}^2(\delta)}\\
&\quad \times\Big\{\frac{\delta^2\lambda^{2\delta}}{\Gamma(2\delta+1)}+2\delta(1-\delta)\frac{\lambda^{\delta}}{\Gamma(\delta+1)}+(1-\delta)^2\Big\}+\ldots,\\
&\bar{\mathbf{U}}(\mathbf{v},\lambda,\varpi)\\
&= (1-\varpi)\exp(\mathbf{v})+\frac{(1-\varpi)(\wp-4)\exp(\mathbf{v})-(1-\varpi)^3\exp(3\mathbf{v})}{\mathbf{N}(\delta)}\Big\{\frac{\delta\lambda^{\delta}}{\Gamma(\delta+1)}+(1-\delta)\Big\}\\
&\quad +\frac{(\varpi-1)(\wp-4)^2\exp(\mathbf{v})-(112-4\wp)(1-\varpi)^3\exp(3\mathbf{v})+30(\varpi-1)^5\exp(5\mathbf{v})}{\mathbf{N}^2(\delta)}\\
&\quad \times\Big\{\frac{\delta^2\lambda^{2\delta}}{\Gamma(2\delta+1)}+2\delta(1-\delta)\frac{\lambda^{\delta}}{\Gamma(\delta+1)}+(1-\delta)^2\Big\}+\ldots.
\end{aligned}
\tag{4.6}
$$

Figure 1 illustrates the influence of 2D and various 3D visualizations for Example 4.1, which is connected to the ABC and Elzaki transform via a fuzzy system in this evaluation. The variability in $\tilde{\mathbf{U}}(\mathbf{v}, \lambda; \varpi)$ on the space coordinate $\mathbf{v}$ with respect to λ and the ambiguity factor $\varpi \in [0, 1]$ is impressively revealed by the explanation.

• The study reveals that the depiction of $\tilde{\mathbf{U}}(\mathbf{v}, \lambda; \varpi)$ will become highly complicated as time progresses.

• Figure 2 illustrates the mapping performance of the proposed technique, $\tilde{\mathbf{U}}(\mathbf{v}, \lambda; \varpi)$, using the fixed variable $\wp = 5$. The report demonstrates that the reduction in $\bar{\mathbf{U}}(\mathbf{v}, \lambda; \varpi)$ correlates with a small boost in $\underline{\mathbf{U}}(\mathbf{v}, \lambda; \varpi)$.

• Figure 2 depicts the performance of the provided fuzzy fractional mapping under the conditions of multiple ambiguity factors for the mappings $\underline{\mathbf{U}}(\mathbf{v}, \lambda; \varpi)$ and $\bar{\mathbf{U}}(\mathbf{v}, \lambda; \varpi)$.

• Figures 1 and 2 demonstrate how to interpret the probabilistic patterns of spatial and temporal variability. Additionally, by employing a inferential statistical assessment, leading scientists in research image generation hypotheses, optics engineering, and stochastic interplay will be able to evaluate effectiveness. Consequently, as the convergence rate increases, the ambiguity factor can help to enhance the findings.

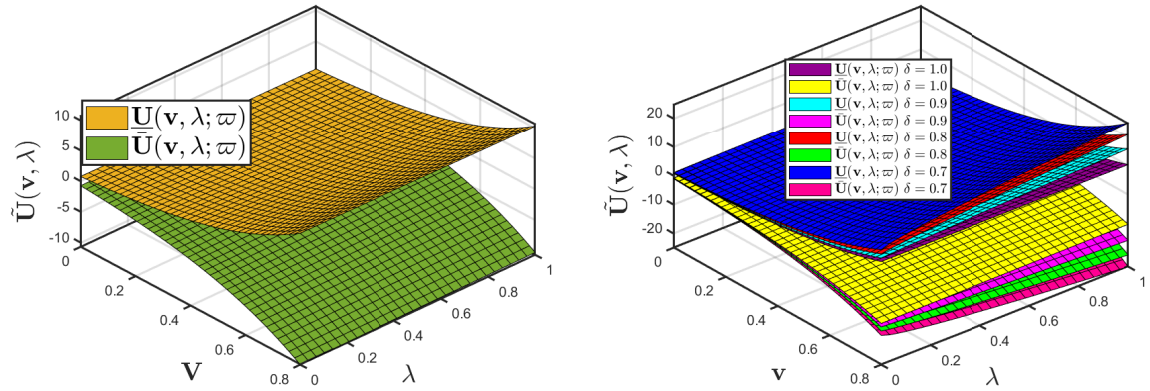

(a) **(b)**

Figure 1. (a) Fuzzy EADM-provided 3D-illustrations of Example 4.1 when $\delta = 1$; (b) Fuzzy EADM-provided 3D-illustrations of multiple profiles of Example 4.1 given $\wp = 5, \mathbf{v}$, and $\varpi \in [0, 1]$.

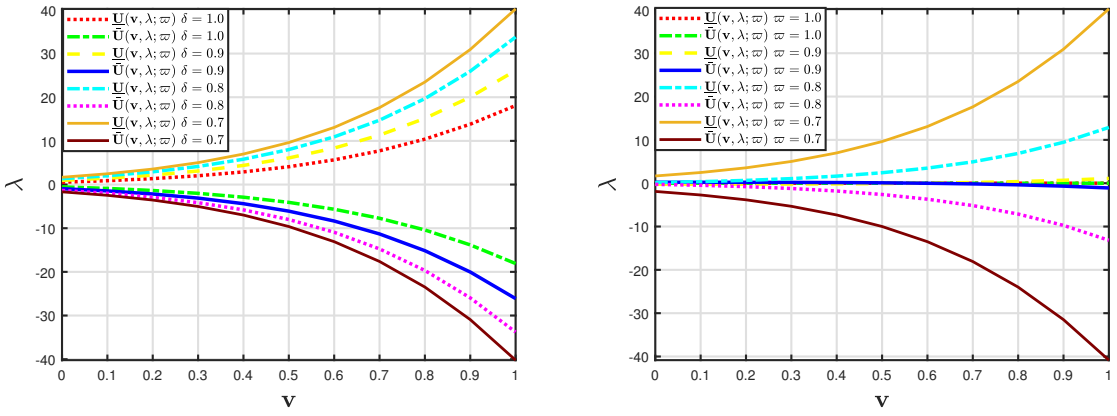

(a) **(b)**

Figure 2. (a) Fuzzy EADM-provided 2D-illustrations of multiple profiles of Example 4.1 when $\varpi = 0.5$ and $\wp = 5$; (b) Fuzzy EADM-provided 2D-illustrations of multiple profiles of Example 4.1 when $\delta = 0.7$ *and* $\lambda = 0.5$.

Remark 4.1. If $\varpi - 1 = 1 - \varpi = 1$ and $\delta = 1$, then Eq (4.6) converges to the exact solution proposed in [39, 40].

Example 4.2. Suppose that the fuzzy fractional-order SHM has fuzzy ICs

$$\begin{aligned}&\frac{\partial^{\delta}}{\partial\lambda^{\delta}}\tilde{\mathbf{U}}(\mathbf{v},\lambda;\varpi) = (\wp-1)\odot\tilde{\mathbf{U}}(\mathbf{v},\lambda;\varpi)\ominus\frac{\partial^{4}}{\partial\mathbf{v}^{4}}\tilde{\mathbf{U}}(\mathbf{v},\lambda;\varpi)\ominus 2\odot\frac{\partial^{2}}{\partial\mathbf{v}^{2}}\tilde{\mathbf{U}}(\mathbf{v},\lambda;\varpi)\ominus\tilde{\mathbf{U}}^{3}(\mathbf{v},\lambda;\varpi),\\&\tilde{\mathbf{U}}(\mathbf{v},0) = \tilde{\Upsilon}(\varpi)\odot\sin\mathbf{v},\end{aligned}\tag{4.7}$$

where $\tilde{\Upsilon}(\varpi) = [\underline{\Upsilon}(\varpi), \bar{\Upsilon}(\varpi)] = [\varpi - 1, 1 - \varpi]$ and there is a fuzzy number $\varpi \in [0, 1]$.

The parametric form of Eq (4.7) is presented as:

$$\begin{cases}\frac{\partial^{\delta}}{\partial\lambda^{\delta}}\underline{\mathbf{U}}(\mathbf{v},\lambda;\varpi) = (\wp-1)\underline{\mathbf{U}}(\mathbf{v},\lambda;\varpi) - \frac{\partial^{4}}{\partial\mathbf{v}^{4}}\underline{\mathbf{U}}(\mathbf{v},\lambda;\varpi) - 2\frac{\partial^{2}}{\partial\mathbf{v}^{2}}\underline{\mathbf{U}}(\mathbf{v},\lambda;\varpi) - \underline{\mathbf{U}}^{3}(\mathbf{v},\lambda;\varpi),\\ \underline{\mathbf{U}}(\mathbf{v},0) = \underline{\Upsilon}(\varpi)\sin\mathbf{v},\\ \frac{\partial^{\delta}}{\partial\lambda^{\delta}}\bar{\mathbf{U}}(\mathbf{v},\lambda;\varpi) = (\wp-1)\bar{\mathbf{U}}(\mathbf{v},\lambda;\varpi) - \frac{\partial^{4}}{\partial\mathbf{v}^{4}}\bar{\mathbf{U}}(\mathbf{v},\lambda;\varpi) - 2\frac{\partial^{2}}{\partial\mathbf{v}^{2}}\bar{\mathbf{U}}(\mathbf{v},\lambda;\varpi) - \bar{\mathbf{U}}^{3}(\mathbf{v},\lambda;\varpi),\\ \bar{\mathbf{U}}(\mathbf{v},0) = \bar{\Upsilon}(\varpi)\sin\mathbf{v}.\end{cases}\tag{4.8}$$

We examine the first instance of Eq (4.8) in an attempt to determine the EADM solution. In view of the procedure outlined in Section 3, we have

$$\begin{aligned}&\frac{\mathbf{N}(\delta)}{1-\delta+\delta\varphi^{\delta}}\mathbb{E}[\underline{\mathbf{U}}(\mathbf{v},\lambda;\varpi)] - \frac{\varphi^{2}\mathbf{N}(\delta)}{1-\delta+\delta\varphi^{\delta}}\underline{\mathbf{U}}_{(\kappa)}(\mathbf{v};\varpi)\\&= \mathbb{E}\left[(\wp-1)\underline{\mathbf{U}}(\mathbf{v},\lambda;\varpi) - \frac{\partial^{4}}{\partial\mathbf{v}^{4}}\underline{\mathbf{U}}(\mathbf{v},\lambda;\varpi) - 2\frac{\partial^{2}}{\partial\mathbf{v}^{2}}\underline{\mathbf{U}}(\mathbf{v},\lambda;\varpi) - \underline{\mathbf{U}}^{3}(\mathbf{v},\lambda;\varpi)\right],\end{aligned}$$

Simple calculations show

$$\underline{\mathbf{U}}(\mathbf{v},\lambda;\varpi) \quad = (\varpi-1)\sin\mathbf{v} + \mathbb{E}^{-1}\left[\frac{1-\delta+\delta\varphi^{\delta}}{\mathbf{N}(\delta)}\right.$$

$$\times\mathbb{E}\Big[(\wp-1)\underline{\mathbf{U}}(\mathbf{v},\lambda;\varpi)-\frac{\partial^4}{\partial\mathbf{v}^4}\underline{\mathbf{U}}(\mathbf{v},\lambda;\varpi)-2\frac{\partial^2}{\partial\mathbf{v}^2}\underline{\mathbf{U}}(\mathbf{v},\lambda;\varpi)-\underline{\mathbf{U}}^3(\mathbf{v},\lambda;\varpi)\Big]\Big]. \quad (4.9)$$

We assume the infinite sum $\underline{\mathbf{U}}(\mathbf{v},\lambda;\varpi)=\sum\limits_{q=0}^{\infty}\underline{\mathbf{U}}_q(\mathbf{v},\lambda;\varpi)$ incorporates Eq (3.5) and validates the non-linearity. As a result, Eq (4.9) leads to the formation

$$\begin{aligned}\sum_{q=0}^{\infty}\underline{\mathbf{U}}_q(\mathbf{v},\lambda;\varpi) &= (\varpi-1)\exp(\mathbf{v})+\mathbb{E}^{-1}\Big[\frac{1-\delta+\delta\varphi^{\delta}}{\mathbf{N}(\delta)}\\ &\times\mathbb{E}\Big[(\wp-1)\sum_{q=0}^{\infty}\underline{\mathbf{U}}_q(\mathbf{v},\lambda;\varpi)-\frac{\partial^4}{\partial\mathbf{v}^4}\sum_{q=0}^{\infty}\underline{\mathbf{U}}_q(\mathbf{v},\lambda;\varpi)-2\frac{\partial^2}{\partial\mathbf{v}^2}\sum_{q=0}^{\infty}\underline{\mathbf{U}}_q(\mathbf{v},\lambda;\varpi)\\ &-\sum_{q=0}^{\infty}\underline{\mathbf{A}}_q(\mathbf{v},\lambda;\varpi)\Big]\Big].\end{aligned} \quad (4.10)$$

By virtue of Eq (4.5), then (4.10) diminishes to

$$\begin{aligned}\underline{\mathbf{U}_0}(\mathbf{v},\lambda;\varpi) &= (\varpi-1)\sin\mathbf{v},\\ \underline{\mathbf{U}_1}(\mathbf{v},\lambda;\varpi) &= \mathbb{E}^{-1}\Big[\frac{1-\delta+\delta\varphi^{\delta}}{\mathbf{N}(\delta)}\mathbb{E}\Big[(\wp-1)\underline{\mathbf{U}}_0(\mathbf{v},\lambda;\varpi)-\frac{\partial^4}{\partial\mathbf{v}^4}\underline{\mathbf{U}}_0(\mathbf{v},\lambda;\varpi)-2\frac{\partial^2}{\partial\mathbf{v}^2}\underline{\mathbf{U}}_0(\mathbf{v},\lambda;\varpi)\\ &\quad-\underline{\mathbf{A}}_0(\mathbf{v},\lambda;\varpi)\Big]\Big]\\ &= \frac{\wp(\varpi-1)\sin\mathbf{v}-(\varpi-1)^3\sin^3\mathbf{v}}{\mathbf{N}(\delta)}\Big\{\frac{\delta\lambda^{\delta}}{\Gamma(\delta+1)}+(1-\delta)\Big\},\\ \underline{\mathbf{U}_2}(\mathbf{v},\lambda;\varpi) &= \mathbb{E}^{-1}\Big[\frac{1-\delta+\delta\varphi^{\delta}}{\mathbf{N}(\delta)}\mathbb{E}\Big[(\wp-1)\underline{\mathbf{U}}_1(\mathbf{v},\lambda;\varpi)-\frac{\partial^4}{\partial\mathbf{v}^4}\underline{\mathbf{U}}_1(\mathbf{v},\lambda;\varpi)-2\frac{\partial^2}{\partial\mathbf{v}^2}\underline{\mathbf{U}}_1(\mathbf{v},\lambda;\varpi)\\ &\quad-\underline{\mathbf{A}}_1(\mathbf{v},\lambda;\varpi)\Big]\Big]\\ &= \frac{\wp^2(\varpi-1)\sin\mathbf{v}-2(2\wp+7)(\varpi-1)^3\sin^3\mathbf{v}-48(\varpi-1)^3\cos^2\mathbf{v}\sin\mathbf{v}+3(\varpi-1)^5\sin^5\mathbf{v}}{\mathbf{N}^2(\delta)}\\ &\quad\times\Big\{\frac{\delta^2\lambda^{2\delta}}{\Gamma(2\delta+1)}+2\delta(1-\delta)\frac{\lambda^{\delta}}{\Gamma(\delta+1)}+(1-\delta)^2\Big\},\\ &\vdots.\end{aligned}$$

In a similar way, additional elements of the EADM system $\underline{\mathbf{U}}q$ ($q\geq 3$) can be identified. Furthermore, as the iterative technique develops, the attained result's trustworthiness improves significantly and the established result appears progressively comparable to the expressive context. As a result, we have formulated a set of solutions that are structured in a series of formulations; that is,

$$\tilde{\mathbf{U}}(\mathbf{v},\lambda,\varpi)=\tilde{\mathbf{U}}_0(\mathbf{v},\lambda,\varpi)+\tilde{\mathbf{U}}_1(\mathbf{v},\lambda,\varpi)+\tilde{\mathbf{U}}_1(\mathbf{v},\lambda,\varpi)+...$$

such that

$$\underline{\mathbf{U}}(\mathbf{v},\lambda,\varpi) = \underline{\mathbf{U}}_0(\mathbf{v},\lambda,\varpi)+\underline{\mathbf{U}}_1(\mathbf{v},\lambda,\varpi)+\underline{\mathbf{U}}_1(\mathbf{v},\lambda,\varpi)+...,$$

$$\bar{\mathbf{U}}(\mathbf{v},\lambda,\varpi) \quad = \bar{\mathbf{U}}_0(\mathbf{v},\lambda,\varpi)+\bar{\mathbf{U}}_1(\mathbf{v},\lambda,\varpi)+\bar{\mathbf{U}}_1(\mathbf{v},\lambda,\varpi)+\dots\,.$$

Eventually, we get

$$\begin{aligned}
\underline{\mathbf{U}}(\mathbf{v},\lambda,\varpi) \quad &= (\varpi-1)\sin\mathbf{v}+\frac{1}{\mathbf{N}(\delta)}\Big[\wp(\varpi-1)\sin\mathbf{v}-(\varpi-1)^3\sin^3\mathbf{v}\Big]\Big\{\frac{\delta\lambda^\delta}{\Gamma(\delta+1)}+(1-\delta)\Big\}\\
&+\frac{1}{\mathbf{N}^2(\delta)}\Big[\wp^2(\varpi-1)\sin\mathbf{v}-2(2\wp+7)(\varpi-1)^3\sin^3\mathbf{v}\\
&\quad -48(\varpi-1)^3\cos^2\mathbf{v}\sin\mathbf{v}+3(\varpi-1)^5\sin^5\mathbf{v}\Big]\\
&\quad \times\Big\{\frac{\delta^2\lambda^{2\delta}}{\Gamma(2\delta+1)}+2\delta(1-\delta)\frac{\lambda^\delta}{\Gamma(\delta+1)}+(1-\delta)^2\Big\}+\dots\,,\\
\bar{\mathbf{U}}(\mathbf{v},\lambda,\varpi) \quad &= (1-\varpi)\sin\mathbf{v}+\frac{1}{\mathbf{N}(\delta)}\Big[\wp(1-\varpi)\sin\mathbf{v}-(1-\varpi)^3\sin^3\mathbf{v}\Big]\Big\{\frac{\delta\lambda^\delta}{\Gamma(\delta+1)}+(1-\delta)\Big\}\\
&+\frac{1}{\mathbf{N}^2(\delta)}\Big[\wp^2(1-\varpi)\sin\mathbf{v}-2(2\wp+7)(1-\varpi)^3\sin^3\mathbf{v}\\
&\quad -48(1-\varpi)^3\cos^2\mathbf{v}\sin\mathbf{v}+3(1-\varpi)^5\sin^5\mathbf{v}\Big]\\
&\quad \times\Big\{\frac{\delta^2\lambda^{2\delta}}{\Gamma(2\delta+1)}+2\delta(1-\delta)\frac{\lambda^\delta}{\Gamma(\delta+1)}+(1-\delta)^2\Big\}+\dots\,.
\end{aligned}\tag{4.11}$$

Figure 3 highlights the implication of two (a) and numerous (b) 3D reconstructions for Example 4.2, which are correlated using the fuzzy fractional ABC and Elzaki transform via fuzzy system in this evaluation. The variability in $\tilde{\mathbf{U}}(\mathbf{v},\lambda;\varpi)$ on the space coordinate $\mathbf{v}$ with respect to λ and the ambiguity factor $\varpi\in[0,1]$ is curiously revealed by the analysis.

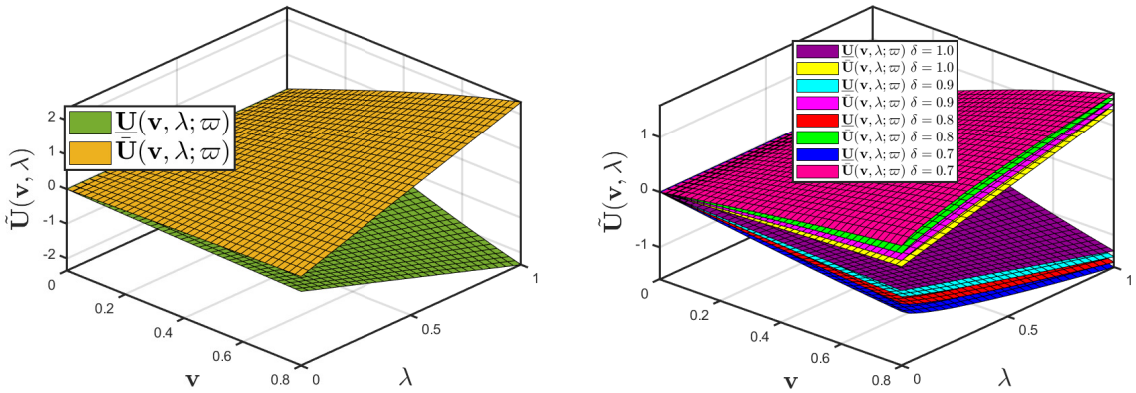

(a) **(b)**

Figure 3. (a) Fuzzy EADM-provided 3D-illustrations of Example 4.2 when $\delta=1$; (b) Fuzzy EADM-provided 3D-illustrations of multiple profiles of Example 4.2 when $\wp=5$ and $\varpi\in[0,1]$.

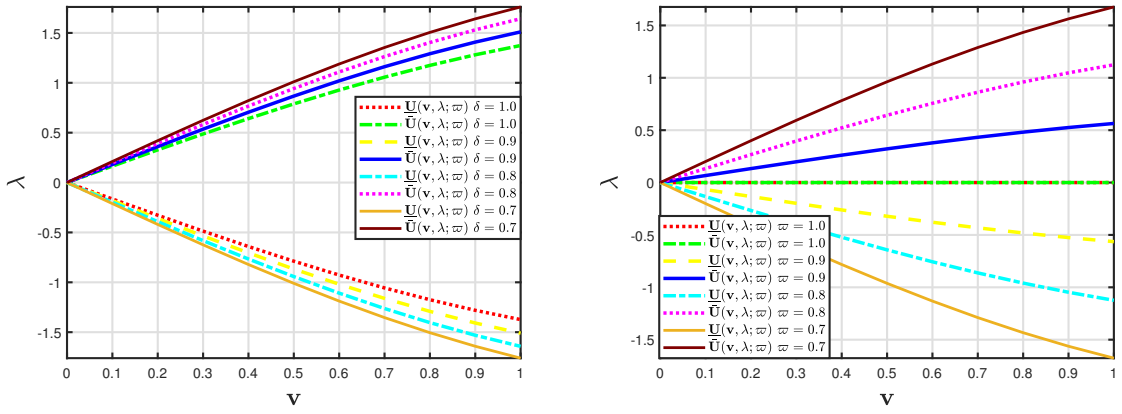

Figure 4. (a) Fuzzy EADM-provided 2D-illustrations of multiple profiles of Example 4.2 when $\varpi = 0.5$, $\lambda = 0.5$ and $\wp = 5$; (b) Fuzzy EADM-provided 2D-illustrations of multiple profiles of Example 4.2 when $\delta = 0.9$ *and* $\lambda = 0.5$.

The investigation revealed that the graphical representation of $\tilde{\mathbf{U}}(\mathbf{v}, \lambda; \varpi)$ will become extremely complicated as time passes.

• Figure 4 displays the mapping accuracy of the proposed technique, $\tilde{\mathbf{U}}(\mathbf{v}, \lambda; \varpi)$, using the consistent parameterization $\wp = 5$. The research has revealed that the reduction in $\bar{\mathbf{U}}(\mathbf{v}, \lambda; \varpi)$ correlates with a modest boost in $\underline{\mathbf{U}}(\mathbf{v}, \lambda; \varpi)$.

• In Figure 4, the ambiguity factors of the transformations $\underline{\mathbf{U}}(\mathbf{v}, \lambda; \varpi)$ and $\bar{\mathbf{U}}(\mathbf{v}, \lambda; \varpi)$ are illustrated; the results specify the performance of prescribed fuzzy fractional mapping for multiple ambiguity factors.

• Figures 3 and 4 exhibit the aforementioned plots, which allow us to explain the probabilistic nature of spatial and temporal variability. Additionally, by employing an inferential statistical assessment, leading researchers in patterning creation research, optical engineering, and probabilistic dynamics will be able to evaluate effectiveness. As a consequence, as the convergence rate increases, the ambiguity component can help to enhance the findings.

Remark 4.2. If $\varpi - 1 = 1 - \varpi = 1$ and $\delta = 1$, then Eq (4.11) converges to the exact solution proposed in [39, 40].

The intention of the following outcome is to leverage Definition 2.11 to establish an analytical solution for the SHM given by Eq (1.2) with propagation.

Example 4.3. Suppose that the fuzzy fractional-order SHM is subject to fuzzy ICs

$$\begin{aligned} \frac{\partial^{\delta}}{\partial \lambda^{\delta}} \tilde{\mathbf{U}}(\mathbf{v}, \lambda; \varpi) &= \epsilon \odot \tilde{\mathbf{U}}(\mathbf{v}, \lambda; \varpi) \oplus 2\tilde{\mathbf{U}}^{2}(\mathbf{v}, \lambda; \varpi) \ominus \tilde{\mathbf{U}}^{3}(\mathbf{v}, \lambda; \varpi) \ominus \frac{\partial^{4}}{\partial \mathbf{v}^{4}} \tilde{\mathbf{U}}(\mathbf{v}, \lambda; \varpi) \\ &\quad \ominus 2 \odot \frac{\partial^{2}}{\partial \mathbf{v}^{2}} \tilde{\mathbf{U}}(\mathbf{v}, \lambda; \varpi) \oplus \eta \odot \frac{\partial^{3}}{\partial \mathbf{v}^{3}} \tilde{\mathbf{U}}(\mathbf{v}, \lambda; \varpi), \\ \tilde{\mathbf{U}}(\mathbf{v}, 0) &= \tilde{\Upsilon}(\varpi) \odot \exp(\mathbf{v}), \end{aligned} \tag{4.12}$$

where $\tilde{\Upsilon}(\varpi) = [\underline{\Upsilon}(\varpi), \bar{\Upsilon}(\varpi)] = [\varpi - 1, 1 - \varpi]$ and there is a fuzzy number $\varpi \in [0, 1]$.

The parameteric form of Eq (4.12) is presented as

$$\begin{cases} \frac{\partial^{\delta}}{\partial\lambda^{\delta}}\underline{\mathbf{U}}(\mathbf{v},\lambda;\varpi) = \epsilon\underline{\mathbf{U}}(\mathbf{v},\lambda;\varpi) + 2\underline{\mathbf{U}}^{2}(\mathbf{v},\lambda;\varpi) - \underline{\mathbf{U}}^{3}(\mathbf{v},\lambda;\varpi) - \frac{\partial^{4}}{\partial\mathbf{v}^{4}}\underline{\mathbf{U}}(\mathbf{v},\lambda;\varpi) \\ \quad -2\frac{\partial^{2}}{\partial\mathbf{v}^{2}}\underline{\mathbf{U}}(\mathbf{v},\lambda;\varpi) + \eta\frac{\partial^{3}}{\partial\mathbf{v}^{3}}\underline{\mathbf{U}}(\mathbf{v},\lambda;\varpi), \\ \underline{\mathbf{U}}(\mathbf{v},0) = \underline{\Upsilon}(\varpi)\exp(\mathbf{v}), \\ \frac{\partial^{\delta}}{\partial\lambda^{\delta}}\bar{\mathbf{U}}(\mathbf{v},\lambda;\varpi) = \epsilon\bar{\mathbf{U}}(\mathbf{v},\lambda;\varpi) + 2\bar{\mathbf{U}}^{2}(\mathbf{v},\lambda;\varpi) - \bar{\mathbf{U}}^{3}(\mathbf{v},\lambda;\varpi) - \frac{\partial^{4}}{\partial\mathbf{v}^{4}}\bar{\mathbf{U}}(\mathbf{v},\lambda;\varpi) \\ \quad -2\frac{\partial^{2}}{\partial\mathbf{v}^{2}}\bar{\mathbf{U}}(\mathbf{v},\lambda;\varpi) + \eta\frac{\partial^{3}}{\partial\mathbf{v}^{3}}\bar{\mathbf{U}}(\mathbf{v},\lambda;\varpi), \\ \bar{\mathbf{U}}(\mathbf{v},0) = \bar{\Upsilon}(\varpi)\exp(\mathbf{v}). \end{cases}$$

We examine the first instance of Eq (4.13) in an attempt to determine the EADM solution. In view of the process outlined in Section 3, we have

$$\begin{aligned} &\frac{\mathbf{N}(\delta)}{1-\delta+\delta\varphi^{\delta}}\mathbb{E}[\underline{\mathbf{U}}(\mathbf{v},\lambda;\varpi)] - \frac{\varphi^{2}\mathbf{N}(\delta)}{1-\delta+\delta\varphi^{\delta}}\underline{\mathbf{U}}_{(\kappa)}(\mathbf{v};\varpi) \\ &= \mathbb{E}\Big[\epsilon\underline{\mathbf{U}}(\mathbf{v},\lambda;\varpi) + 2\underline{\mathbf{U}}^{2}(\mathbf{v},\lambda;\varpi) - \underline{\mathbf{U}}^{3}(\mathbf{v},\lambda;\varpi) - \frac{\partial^{4}}{\partial\mathbf{v}^{4}}\underline{\mathbf{U}}(\mathbf{v},\lambda;\varpi) - 2\frac{\partial^{2}}{\partial\mathbf{v}^{2}}\underline{\mathbf{U}}(\mathbf{v},\lambda;\varpi) \\ &\quad +\eta\frac{\partial^{3}}{\partial\mathbf{v}^{3}}\underline{\mathbf{U}}(\mathbf{v},\lambda;\varpi)\Big]. \end{aligned}$$

Simple calculations show that

$$\begin{aligned} \underline{\mathbf{U}}(\mathbf{v},\lambda;\varpi) \quad &= (\varpi-1)\exp(\mathbf{v}) \\ &\quad +\mathbb{E}^{-1}\left[\frac{1-\delta+\delta\varphi^{\delta}}{\mathbf{N}(\delta)}\mathbb{E}\left\{\begin{array}{l}\epsilon\underline{\mathbf{U}}(\mathbf{v},\lambda;\varpi) + 2\underline{\mathbf{U}}^{2}(\mathbf{v},\lambda;\varpi) - \underline{\mathbf{U}}^{3}(\mathbf{v},\lambda;\varpi) \\ \quad -\frac{\partial^{4}}{\partial\mathbf{v}^{4}}\underline{\mathbf{U}}(\mathbf{v},\lambda;\varpi) - 2\frac{\partial^{2}}{\partial\mathbf{v}^{2}}\underline{\mathbf{U}}(\mathbf{v},\lambda;\varpi) + \eta\frac{\partial^{3}}{\partial\mathbf{v}^{3}}\underline{\mathbf{U}}(\mathbf{v},\lambda;\varpi)\end{array}\right\}\right]. \end{aligned} \tag{4.13}$$

We assume the infinite sum $\underline{\mathbf{U}}(\mathbf{v},\lambda;\varpi) = \sum_{q=0}^{\infty}\underline{\mathbf{U}}_{q}(\mathbf{v},\lambda;\varpi)$ incorporates Eq (3.5) and validates the non-linearity. As a result, Eq (4.13) leads to the formation

$$\begin{aligned} \sum_{q=0}^{\infty}\underline{\mathbf{U}}_{q}(\mathbf{v},\lambda;\varpi) \quad &= (\varpi-1)\exp(\mathbf{v}) + \mathbb{E}^{-1}\frac{1-\delta+\delta\varphi^{\delta}}{\mathbf{N}(\delta)} \\ &\quad \times\mathbb{E}\left\{\begin{array}{l}\epsilon\sum_{q=0}^{\infty}\underline{\mathbf{U}}(\mathbf{v},\lambda;\varpi) + 2\sum_{q=0}^{\infty}\underline{\mathbf{B}}_{q}(\mathbf{v},\lambda;\varpi) - \sum_{q=0}^{\infty}\underline{\mathbf{A}}_{q}(\mathbf{v},\lambda;\varpi) \\ \quad -\frac{\partial^{4}}{\partial\mathbf{v}^{4}}\sum_{q=0}^{\infty}\underline{\mathbf{U}}(\mathbf{v},\lambda;\varpi) - 2\frac{\partial^{2}}{\partial\mathbf{v}^{2}}\sum_{q=0}^{\infty}\underline{\mathbf{U}}(\mathbf{v},\lambda;\varpi) + \eta\frac{\partial^{3}}{\partial\mathbf{v}^{3}}\sum_{q=0}^{\infty}\underline{\mathbf{U}}(\mathbf{v},\lambda;\varpi).\end{array}\right. \end{aligned} \tag{4.14}$$

The foregoing formulae have two non linear factors including $\underline{\mathbf{U}}^{3} = \sum_{q=0}^{\infty}\underline{\mathbf{A}}_{q}$ and $\underline{\mathbf{U}}^{2} = \sum_{q=0}^{\infty}\underline{\mathbf{B}}_{q}$, which can be examined by using the Adomian polynomial Eq (3.4). Thus, in view of Eq (4.5), Adomian polynomials for $\underline{\mathbf{U}}^{2} = \sum_{q=0}^{\infty}\underline{\mathbf{B}}_{q}$ are determined as

$$\underline{\mathbf{B}}_{q}(\underline{\mathbf{U}}^{2}) = \begin{cases}\underline{\mathbf{U}}_{0}^{2}, & q=0, \\ 2\underline{\mathbf{U}}_{0}\underline{\mathbf{U}}_{1}, & q=1, \\ 2\underline{\mathbf{U}}_{0}\underline{\mathbf{U}}_{2} + \underline{\mathbf{U}}_{1}^{2}, & q=2.\end{cases} \tag{4.15}$$

Then, Eq (4.14) diminishes to

$$\begin{aligned}
\underline{\mathbf{U}_0}(\mathbf{v},\lambda;\varpi) &= (\varpi-1)\exp(\mathbf{v}),\\
\underline{\mathbf{U}_1}(\mathbf{v},\lambda;\varpi) &= \mathbb{E}^{-1}\left[\frac{1-\delta+\delta\varphi^{\delta}}{\mathbf{N}(\delta)}\mathbb{E}\left\{\begin{array}{l}\epsilon\underline{\mathbf{U}}_0(\mathbf{v},\lambda;\varpi)+2\underline{\mathbf{B}}_0(\mathbf{v},\lambda;\varpi)-\underline{\mathbf{A}}_0(\mathbf{v},\lambda;\varpi)\\ \quad -\frac{\partial^4}{\partial\mathbf{v}^4}\underline{\mathbf{U}}_0(\mathbf{v},\lambda;\varpi)-2\frac{\partial^2}{\partial\mathbf{v}^2}\underline{\mathbf{U}}_0(\mathbf{v},\lambda;\varpi)+\eta\frac{\partial^3}{\partial\mathbf{v}^3}\underline{\mathbf{U}}_0(\mathbf{v},\lambda;\varpi)\end{array}\right.\right]\\
&= \frac{(\varpi-1)(\epsilon+\eta-3)\exp(\mathbf{v})+2(\varpi-1)^2\exp(2\mathbf{v})-(\varpi-1)^3\exp(3\mathbf{v})}{\mathbf{N}(\delta)}\\
&\quad\times\left\{\frac{\delta\lambda^{\delta}}{\Gamma(\delta+1)}+(1-\delta)\right\},\\
\underline{\mathbf{U}_2}(\mathbf{v},\lambda;\varpi) &= \mathbb{E}^{-1}\left[\frac{1-\delta+\delta\varphi^{\delta}}{\mathbf{N}(\delta)}\mathbb{E}\left\{\begin{array}{l}\epsilon\underline{\mathbf{U}}_1(\mathbf{v},\lambda;\varpi)+2\underline{\mathbf{B}}_1(\mathbf{v},\lambda;\varpi)-\underline{\mathbf{A}}_1(\mathbf{v},\lambda;\varpi)\\ \quad -\frac{\partial^4}{\partial\mathbf{v}^4}\underline{\mathbf{U}}_1(\mathbf{v},\lambda;\varpi)-2\frac{\partial^2}{\partial\mathbf{v}^2}\underline{\mathbf{U}}_1(\mathbf{v},\lambda;\varpi)+\eta\frac{\partial^3}{\partial\mathbf{v}^3}\underline{\mathbf{U}}_1(\mathbf{v},\lambda;\varpi)\end{array}\right.\right]\\
&= \frac{1}{\mathbf{N}^2(\delta)}\left\{\frac{\delta^2\lambda^{2\delta}}{\Gamma(2\delta+1)}+2\delta(1-\delta)\frac{\lambda^{\delta}}{\Gamma(\delta+1)}+(1-\delta)^2\right\}\\
&\quad\times\left\{\begin{array}{l}(\epsilon^2+\eta^2-6(\epsilon+\eta)+2\epsilon\eta+9)(\varpi-1)\exp(\mathbf{v})+(\varpi-1)^2\exp(2\mathbf{v})\\ \quad\times(20\eta+6\epsilon-60)+(\varpi-1)^3\exp(3\mathbf{v})(116-4\epsilon-30\eta)\\ \quad -10(\varpi-1)^4\exp(4\mathbf{v})+3(\varpi-1)^5\exp(5\mathbf{v}),\end{array}\right.\\
&\vdots .
\end{aligned}$$

In a similar way, additional elements of the EADM system $\underline{\mathbf{U}}q$ ($q \geq 3$) can be identified. Furthermore, as the iterative technique develops, the attained result's trustworthiness improves significantly and the established result appears progressively comparable to the expressive context. As a result, we have formulated a set of solutions that are structured in a series of formulations; that is,

$$\tilde{\mathbf{U}}(\mathbf{v},\lambda,\varpi) = \tilde{\mathbf{U}}_0(\mathbf{v},\lambda,\varpi)+\tilde{\mathbf{U}}_1(\mathbf{v},\lambda,\varpi)+\tilde{\mathbf{U}}_1(\mathbf{v},\lambda,\varpi)+\ldots$$

such that

$$\begin{aligned}
\underline{\mathbf{U}}(\mathbf{v},\lambda,\varpi) &= \underline{\mathbf{U}}_0(\mathbf{v},\lambda,\varpi)+\underline{\mathbf{U}}_1(\mathbf{v},\lambda,\varpi)+\underline{\mathbf{U}}_1(\mathbf{v},\lambda,\varpi)+\ldots,\\
\bar{\mathbf{U}}(\mathbf{v},\lambda,\varpi) &= \bar{\mathbf{U}}_0(\mathbf{v},\lambda,\varpi)+\bar{\mathbf{U}}_1(\mathbf{v},\lambda,\varpi)+\bar{\mathbf{U}}_1(\mathbf{v},\lambda,\varpi)+\ldots.
\end{aligned}$$

Eventually, we get

$$\begin{aligned}
\underline{\mathbf{U}}(\mathbf{v},\lambda,\varpi) &= (\varpi-1)\exp(\mathbf{v})\\
&+\frac{1}{\mathbf{N}(\delta)}\Big[(\varpi-1)(\epsilon+\eta-3)\exp(\mathbf{v})+2(\varpi-1)^2\exp(2\mathbf{v})-(\varpi-1)^3\exp(3\mathbf{v})\Big]\\
&\times\left\{\frac{\delta\lambda^{\delta}}{\Gamma(\delta+1)}+(1-\delta)\right\}\\
&+\frac{1}{\mathbf{N}^2(\delta)}\left\{\frac{\delta^2\lambda^{2\delta}}{\Gamma(2\delta+1)}+2\delta(1-\delta)\frac{\lambda^{\delta}}{\Gamma(\delta+1)}+(1-\delta)^2\right\}\\
&\times\left\{\begin{array}{l}(\epsilon^2+\eta^2-6(\epsilon+\eta)+2\epsilon\eta+9)(\varpi-1)\exp(\mathbf{v})+(\varpi-1)^2\exp(2\mathbf{v})(20\eta+6\epsilon-60)\\ \quad +(\varpi-1)^3\exp(3\mathbf{v})(116-4\epsilon-30\eta)-10(\varpi-1)^4\exp(4\mathbf{v})+3(\varpi-1)^5\exp(5\mathbf{v})\end{array}\right.
\end{aligned}$$

$$
\begin{aligned}
&+\dots,\\
\bar{\mathbf{U}}(\mathbf{v},\lambda,\varpi) &= (1-\varpi)\exp(\mathbf{v})\\
&+\frac{1}{\mathbf{N}(\delta)}\Big[(1-\varpi)(\epsilon+\eta-3)\exp(\mathbf{v})+2(1-\varpi)^2\exp(2\mathbf{v})-(1-\varpi)^3\exp(3\mathbf{v})\Big]\\
&\times\left\{\frac{\delta\lambda^{\delta}}{\Gamma(\delta+1)}+(1-\delta)\right\}\\
&+\frac{1}{\mathbf{N}^2(\delta)}\left\{\frac{\delta^2\lambda^{2\delta}}{\Gamma(2\delta+1)}+2\delta(1-\delta)\frac{\lambda^{\delta}}{\Gamma(\delta+1)}+(1-\delta)^2\right\}\\
&\times\begin{Bmatrix}(\epsilon^2+\eta^2-6(\epsilon+\eta)+2\epsilon\eta+9)(1-\varpi)\exp(\mathbf{v})+(1-\varpi)^2\exp(2\mathbf{v})(20\eta+6\epsilon-60)\\ \quad+(1-\varpi)^3\exp(3\mathbf{v})(116-4\epsilon-30\eta)-10(1-\varpi)^4\exp(4\mathbf{v})+3(1-\varpi)^5\exp(5\mathbf{v})\end{Bmatrix}\\
&+\dots. \qquad (4.16)
\end{aligned}
$$

Figure 5 shows the effects of two (a) and various (b) 3D illustrations for Example 4.3 under the conditions of applying the fractional ABC and Elzaki transform via fuzzy system in this evaluation. The deviations in $\tilde{\mathbf{U}}(\mathbf{v},\lambda;\varpi)$ on the space coordinate $\mathbf{v}$ with respect to λ and the ambiguity factor $\varpi\in[0,1]$ are impressively highlighted by the discussion. The exploration illustrates that the representation of $\tilde{\mathbf{U}}(\mathbf{v},\lambda;\varpi)$ will emerge to be progressively intricate as time passes.

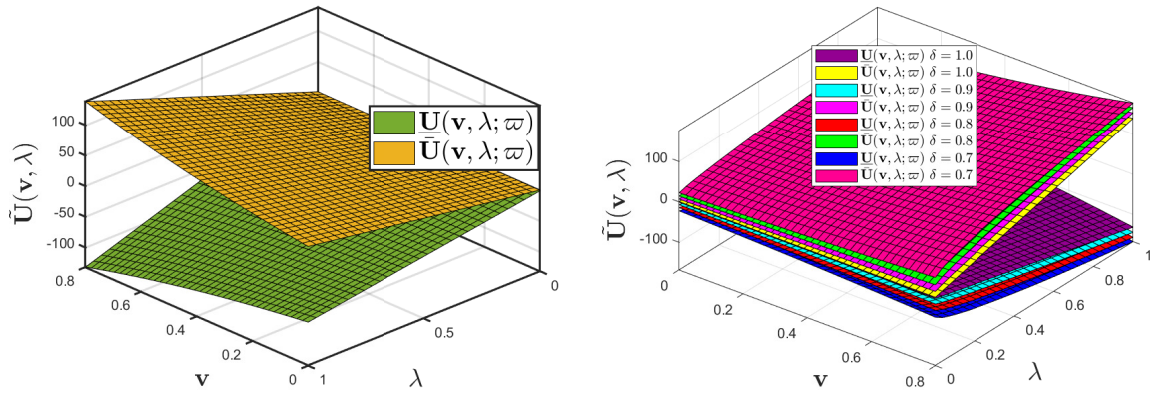

(a) **(b)**

Figure 5. (a) Fuzzy EADM-provided 3D-illustrations of Example 4.3 when $\delta=1$, $\epsilon=5$ and $\eta=10$ (b) Fuzzy EADM-provided 3D-illustrations of multiple profiles of Example 4.3 when $\epsilon=5,\eta=10$ and $\varpi\in[0,1]$.

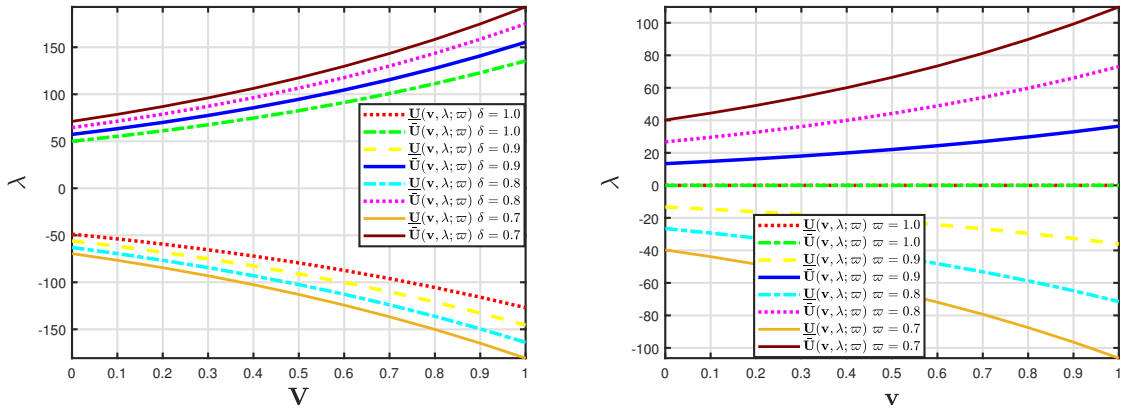

Figure 6. (a) Fuzzy EADM-provided 2D-illustrations of multiple profiles of Example 4.3 when $\varpi = 0.9$, $\epsilon = 10$ and $\eta = 3$ with $\lambda = 0.5$; (b) Fuzzy EADM-provided 2D-illustrations of multiple profiles of Example 4.3 when $\delta = 0.9$ *and* $\lambda = 0.5$ with varying fractional-order.

• Figure 6 depicts the mapping performance of the proposed methodology, $\tilde{\mathbf{U}}(\mathbf{v}, \lambda; \varpi)$, with the control variables $\eta = 10$ and $\epsilon = 5$. The study indicates that the reduction in $\bar{\mathbf{U}}(\mathbf{v}, \lambda; \varpi)$ translates to a slight increase in $\underline{\mathbf{U}}(\mathbf{v}, \lambda; \varpi)$.
• In Figure 6, the ambiguity components of the transformations $\underline{\mathbf{U}}(\mathbf{v}, \lambda; \varpi)$ and $\bar{\mathbf{U}}(\mathbf{v}, \lambda; \varpi)$ are exhibited; the results demonstrate the conduct of the prescribed fuzzy fractional-order of the mapping for multiple ambiguity factors.
• Figures 5 and 6 depict the preceding plots, which allow us to explain the probabilistic nature of spatial and temporal fluctuations. However, by employing the appropriate statistical analysis, researchers specializing in pattern development hypotheses, optical engineering and probabilistic kinetics will be able to evaluate productivity. As a consequence, improved simulations of fluid mechanics instability with bifurcated and diffraction characteristics are achievable.

Remark 4.3. If $\varpi - 1 = 1 - \varpi = 1$ and $\delta = 1$, then Eq (4.16) converges to the exact solution proposed in [39, 40].

Example 4.4. Suppose that the fuzzy fractional-order SHM is subject to fuzzy ICs

$$\begin{aligned} \frac{\partial^{\delta}}{\partial \lambda^{\delta}} \tilde{\mathbf{U}}(\mathbf{v}, \lambda; \varpi) \quad &= \epsilon \odot \tilde{\mathbf{U}}(\mathbf{v}, \lambda; \varpi) \oplus 2 \odot \tilde{\mathbf{U}}^{2}(\mathbf{v}, \lambda; \varpi) \ominus \tilde{\mathbf{U}}^{3}(\mathbf{v}, \lambda; \varpi) \ominus \frac{\partial^{4}}{\partial \mathbf{v}^{4}} \tilde{\mathbf{U}}(\mathbf{v}, \lambda; \varpi) \\ &\ominus 2 \odot \frac{\partial^{2}}{\partial \mathbf{v}^{2}} \tilde{\mathbf{U}}(\mathbf{v}, \lambda; \varpi) \oplus \eta \odot \frac{\partial^{3}}{\partial \mathbf{v}^{3}} \tilde{\mathbf{U}}(\mathbf{v}, \lambda; \varpi), \\ \tilde{\mathbf{U}}(\mathbf{v}, 0) &= \tilde{\Upsilon}(\varpi) \odot \cos \mathbf{v}, \end{aligned} \tag{4.17}$$

where $\tilde{\Upsilon}(\varpi) = [\underline{\Upsilon}(\varpi), \bar{\Upsilon}(\varpi)] = [\varpi - 1, 1 - \varpi]$ and there is a fuzzy number $\varpi \in [0, 1]$.

The parametric form of Eq (4.17) is presented as

$$\begin{cases} \frac{\partial^{\delta}}{\partial\lambda^{\delta}}\underline{\mathbf{U}}(\mathbf{v},\lambda;\varpi) = \epsilon\underline{\mathbf{U}}(\mathbf{v},\lambda;\varpi) + 2\underline{\mathbf{U}}^{2}(\mathbf{v},\lambda;\varpi) - \underline{\mathbf{U}}^{3}(\mathbf{v},\lambda;\varpi) - \frac{\partial^{4}}{\partial\mathbf{v}^{4}}\underline{\mathbf{U}}(\mathbf{v},\lambda;\varpi) \\ \quad -2\frac{\partial^{2}}{\partial\mathbf{v}^{2}}\underline{\mathbf{U}}(\mathbf{v},\lambda;\varpi) + \eta\frac{\partial^{3}}{\partial\mathbf{v}^{3}}\underline{\mathbf{U}}(\mathbf{v},\lambda;\varpi), \\ \underline{\mathbf{U}}(\mathbf{v},0) = \underline{\Upsilon}(\varpi)\cos\mathbf{v}, \\ \frac{\partial^{\delta}}{\partial\lambda^{\delta}}\bar{\mathbf{U}}(\mathbf{v},\lambda;\varpi) = \epsilon\bar{\mathbf{U}}(\mathbf{v},\lambda;\varpi) + 2\bar{\mathbf{U}}^{2}(\mathbf{v},\lambda;\varpi) - \bar{\mathbf{U}}^{3}(\mathbf{v},\lambda;\varpi) - \frac{\partial^{4}}{\partial\mathbf{v}^{4}}\bar{\mathbf{U}}(\mathbf{v},\lambda;\varpi) \\ \quad -2\frac{\partial^{2}}{\partial\mathbf{v}^{2}}\bar{\mathbf{U}}(\mathbf{v},\lambda;\varpi) + \eta\frac{\partial^{3}}{\partial\mathbf{v}^{3}}\bar{\mathbf{U}}(\mathbf{v},\lambda;\varpi), \\ \bar{\mathbf{U}}(\mathbf{v},0) = \bar{\Upsilon}(\varpi)\cos\mathbf{v}. \end{cases}$$

We examine the first instance of Eq (4.18) in an attempt to determine the EADM solution. In view of the procedure outlined in Section 3, we have

$$\begin{aligned} &\frac{\mathbf{N}(\delta)}{1-\delta+\delta\varphi^{\delta}}\mathbb{E}[\underline{\mathbf{U}}(\mathbf{v},\lambda;\varpi)] - \frac{\varphi^{2}\mathbf{N}(\delta)}{1-\delta+\delta\varphi^{\delta}}\underline{\mathbf{U}}_{(\kappa)}(\mathbf{v};\varpi) \\ &= \mathbb{E}\Big[\epsilon\underline{\mathbf{U}}(\mathbf{v},\lambda;\varpi) + 2\underline{\mathbf{U}}^{2}(\mathbf{v},\lambda;\varpi) - \underline{\mathbf{U}}^{3}(\mathbf{v},\lambda;\varpi) - \frac{\partial^{4}}{\partial\mathbf{v}^{4}}\underline{\mathbf{U}}(\mathbf{v},\lambda;\varpi) - 2\frac{\partial^{2}}{\partial\mathbf{v}^{2}}\underline{\mathbf{U}}(\mathbf{v},\lambda;\varpi) \\ &\quad +\eta\frac{\partial^{3}}{\partial\mathbf{v}^{3}}\underline{\mathbf{U}}(\mathbf{v},\lambda;\varpi)\Big]. \end{aligned}$$

Simple calculations show that

$$\begin{aligned} \underline{\mathbf{U}}(\mathbf{v},\lambda;\varpi) \quad &= (\varpi-1)\cos\mathbf{v} + \mathbb{E}^{-1}\Bigg[\frac{1-\delta+\delta\varphi^{\delta}}{\mathbf{N}(\delta)} \\ &\quad \times\mathbb{E}\begin{cases} \epsilon\underline{\mathbf{U}}(\mathbf{v},\lambda;\varpi) + 2\underline{\mathbf{U}}^{2}(\mathbf{v},\lambda;\varpi) - \underline{\mathbf{U}}^{3}(\mathbf{v},\lambda;\varpi) - \frac{\partial^{4}}{\partial\mathbf{v}^{4}}\underline{\mathbf{U}}(\mathbf{v},\lambda;\varpi) \\ -2\frac{\partial^{2}}{\partial\mathbf{v}^{2}}\underline{\mathbf{U}}(\mathbf{v},\lambda;\varpi) + \eta\frac{\partial^{3}}{\partial\mathbf{v}^{3}}\underline{\mathbf{U}}(\mathbf{v},\lambda;\varpi) \end{cases}\Bigg]. \end{aligned} \tag{4.18}$$

We assume the infinite sum $\underline{\mathbf{U}}(\mathbf{v},\lambda;\varpi) = \sum_{q=0}^{\infty}\underline{\mathbf{U}}_{q}(\mathbf{v},\lambda;\varpi)$ incorporates Eq (3.5) and validates the non-linearity. As a result, Eq (4.18) leads to the formation

$$\begin{aligned} \sum_{q=0}^{\infty}\underline{\mathbf{U}}_{q}(\mathbf{v},\lambda;\varpi) \quad &= (\varpi-1)\cos\mathbf{v} \\ &\quad +\mathbb{E}^{-1}\Bigg[\frac{1-\delta+\delta\varphi^{\delta}}{\mathbf{N}(\delta)}\mathbb{E}\begin{cases} \epsilon\sum_{q=0}^{\infty}\underline{\mathbf{U}}(\mathbf{v},\lambda;\varpi) + 2\sum_{q=0}^{\infty}\underline{\mathbf{B}}_{q}(\mathbf{v},\lambda;\varpi) - \sum_{q=0}^{\infty}\underline{\mathbf{A}}_{q}(\mathbf{v},\lambda;\varpi) \\ -\frac{\partial^{4}}{\partial\mathbf{v}^{4}}\sum_{q=0}^{\infty}\underline{\mathbf{U}}(\mathbf{v},\lambda;\varpi) - 2\frac{\partial^{2}}{\partial\mathbf{v}^{2}}\sum_{q=0}^{\infty}\underline{\mathbf{U}}(\mathbf{v},\lambda;\varpi) \\ +\eta\frac{\partial^{3}}{\partial\mathbf{v}^{3}}\sum_{q=0}^{\infty}\underline{\mathbf{U}}(\mathbf{v},\lambda;\varpi) \end{cases}\Bigg]. \end{aligned}$$

The foregoing formulae have two non linear factors including $\underline{\mathbf{U}}^{3} = \sum_{q=0}^{\infty}\underline{\mathbf{A}}_{q}$ and $\underline{\mathbf{U}}^{2} = \sum_{q=0}^{\infty}\underline{\mathbf{B}}_{q}$ which can be examined by using the Adomian polynomial defined by Eq (3.4). Thus, in view of Eq (4.5),

some Adomian polynomials for $\underline{\mathbf{U}}^2 = \sum_{q=0}^{\infty} \underline{\mathbf{B}}_q$ are determined as

$$\underline{\mathbf{B}}_q(\underline{\mathbf{U}}^2) = \begin{cases} \underline{\mathbf{U}}_0^2, & q = 0, \\ 2\underline{\mathbf{U}}_0\underline{\mathbf{U}}_1, & q = 1, \\ 2\underline{\mathbf{U}}_0\underline{\mathbf{U}}_2 + \underline{\mathbf{U}}_1^2, & q = 2. \end{cases} \tag{4.19}$$

Then, (4.19) diminishes to

$$\begin{aligned}
\underline{\mathbf{U}_0}(\mathbf{v},\lambda;\varpi) &= (\varpi-1)\cos\mathbf{v},\\
\underline{\mathbf{U}_1}(\mathbf{v},\lambda;\varpi) &= \mathbb{E}^{-1}\left[\frac{1-\delta+\delta\varphi^{\delta}}{\mathbf{N}(\delta)}\mathbb{E}\left\{\begin{array}{l}\epsilon\underline{\mathbf{U}}_0(\mathbf{v},\lambda;\varpi)+2\underline{\mathbf{B}}_0(\mathbf{v},\lambda;\varpi)-\underline{\mathbf{A}}_0(\mathbf{v},\lambda;\varpi)\\ \quad -\frac{\partial^4}{\partial\mathbf{v}^4}\underline{\mathbf{U}}_0(\mathbf{v},\lambda;\varpi)-2\frac{\partial^2}{\partial\mathbf{v}^2}\underline{\mathbf{U}}_0(\mathbf{v},\lambda;\varpi)+\eta\frac{\partial^3}{\partial\mathbf{v}^3}\underline{\mathbf{U}}_0(\mathbf{v},\lambda;\varpi)\end{array}\right.\right]\\
&= \frac{1}{\mathbf{N}(\delta)}\Big[(\varpi-1)\Big((\epsilon+1)\cos\mathbf{v}+\eta\sin\mathbf{v}\Big)+2(\varpi-1)^2\cos^2\mathbf{v}-(\varpi-1)^3\cos^3\mathbf{v}\Big]\\
&\quad\times\left\{\frac{\delta\lambda^{\delta}}{\Gamma(\delta+1)}+(1-\delta)\right\},\\
\underline{\mathbf{U}_2}(\mathbf{v},\lambda;\varpi) &= \mathbb{E}^{-1}\left[\frac{1-\delta+\delta\varphi^{\delta}}{\mathbf{N}(\delta)}\mathbb{E}\left\{\begin{array}{l}\epsilon\underline{\mathbf{U}}_1(\mathbf{v},\lambda;\varpi)+2\underline{\mathbf{B}}_1(\mathbf{v},\lambda;\varpi)-\underline{\mathbf{A}}_1(\mathbf{v},\lambda;\varpi)\\ \quad -\frac{\partial^4}{\partial\mathbf{v}^4}\underline{\mathbf{U}}_1(\mathbf{v},\lambda;\varpi)-2\frac{\partial^2}{\partial\mathbf{v}^2}\underline{\mathbf{U}}_1(\mathbf{v},\lambda;\varpi)+\eta\frac{\partial^3}{\partial\mathbf{v}^3}\underline{\mathbf{U}}_1(\mathbf{v},\lambda;\varpi)\end{array}\right.\right]\\
&= \frac{1}{\mathbf{N}^2(\delta)}\left\{\frac{\delta^2\lambda^{2\delta}}{\Gamma(2\delta+1)}+2\delta(1-\delta)\frac{\lambda^{\delta}}{\Gamma(\delta+1)}+(1-\delta)^2\right\}\\
&\quad\times\left\{\begin{array}{l}\epsilon\Big((\varpi-1)((\epsilon+1)\cos\mathbf{v}+\eta\sin\mathbf{v})+2(\varpi-1)^2\cos^2\mathbf{v}-(\varpi-1)^3\cos^3\mathbf{v}\Big)\\ \quad+4(\varpi-1)\cos\mathbf{v}\Big((\varpi-1)((\epsilon+1)\cos\mathbf{v}+\eta\sin\mathbf{v})+2(\varpi-1)^2\cos^2\mathbf{v}\\ \quad\times-(\varpi-1)^3\cos^3\mathbf{v}\Big)-3(\varpi-1)\cos^2\mathbf{v}\Big((\varpi-1)((\epsilon+1)\cos\mathbf{v}+\eta\sin\mathbf{v})\\ \quad\times+2(\varpi-1)^2\cos^2\mathbf{v}-(\varpi-1)^3\cos^3\mathbf{v}\Big)-(\varpi-1)((\epsilon+1)\cos\mathbf{v}+\eta\sin\mathbf{v})\\ \quad+24(\varpi-1)^2(\cos^2\mathbf{v}-\sin^2\mathbf{v})+3(\varpi-1)^3(20\cos\mathbf{v}\sin^2\mathbf{v}-7\cos^3\mathbf{v})\\ \quad+2(\varpi-1)((\epsilon+1)\cos\mathbf{v}+\eta\sin\mathbf{v})-6(\varpi-1)^3(\cos^3\mathbf{v}-2\cos\mathbf{v}\sin^2\mathbf{v})\\ \quad+\eta(\varpi-1)((\epsilon+1)\sin\mathbf{v}-\eta\cos\mathbf{v})+16(\varpi-1)^2\cos\mathbf{v}\sin\mathbf{v}+3(\varpi-1)^3\\ \quad\times(2\sin^3\mathbf{v}-7\cos^2\mathbf{v}\sin\mathbf{v})\end{array}\right.\\
&\vdots.
\end{aligned}$$

In a similar way, additional elements of the EADM system $\underline{\mathbf{U}}q$ ($q \geq 3$) can be identified. Furthermore, as the iterative technique develops, the attained result's trustworthiness improves significantly, and the established result appears progressively comparable to the expressive context. As a result, we have formulated a set of solutions that are structured in a series of formulations; that is,

$$\tilde{\mathbf{U}}(\mathbf{v},\lambda,\varpi) = \tilde{\mathbf{U}}_0(\mathbf{v},\lambda,\varpi) + \tilde{\mathbf{U}}_1(\mathbf{v},\lambda,\varpi) + \tilde{\mathbf{U}}_1(\mathbf{v},\lambda,\varpi) + ...$$

such that

$$\underline{\mathbf{U}}(\mathbf{v},\lambda,\varpi) = \underline{\mathbf{U}}_0(\mathbf{v},\lambda,\varpi) + \underline{\mathbf{U}}_1(\mathbf{v},\lambda,\varpi) + \underline{\mathbf{U}}_1(\mathbf{v},\lambda,\varpi) + ...\,,$$

$$\bar{\mathbf{U}}(\mathbf{v},\lambda,\varpi) \quad = \bar{\mathbf{U}}_0(\mathbf{v},\lambda,\varpi) + \bar{\mathbf{U}}_1(\mathbf{v},\lambda,\varpi) + \bar{\mathbf{U}}_1(\mathbf{v},\lambda,\varpi) + \dots .$$

Eventually, we get

$$\begin{aligned}
\underline{\mathbf{U}}(\mathbf{v},\lambda,\varpi) \quad &= (\varpi-1)\cos\mathbf{v} + \frac{1}{\mathbf{N}(\delta)}\Big[(\varpi-1)\Big((\epsilon+1)\cos\mathbf{v}+\eta\sin\mathbf{v}\Big) + 2(\varpi-1)^2\cos^2\mathbf{v} \\
&\quad -(\varpi-1)^3\cos^3\mathbf{v}\Big]\Big\{\frac{\delta\lambda^\delta}{\Gamma(\delta+1)} + (1-\delta)\Big\} \\
&\quad + \frac{1}{\mathbf{N}^2(\delta)}\Big\{\frac{\delta^2\lambda^{2\delta}}{\Gamma(2\delta+1)} + 2\delta(1-\delta)\frac{\lambda^\delta}{\Gamma(\delta+1)} + (1-\delta)^2\Big\} \\
&\quad \times\begin{cases}
\epsilon\Big((\varpi-1)((\epsilon+1)\cos\mathbf{v}+\eta\sin\mathbf{v}) + 2(\varpi-1)^2\cos^2\mathbf{v} \\
\quad -(\varpi-1)^3\cos^3\mathbf{v}\Big) + 4(\varpi-1)\cos\mathbf{v}\Big((\varpi-1)((\epsilon+1)\cos\mathbf{v}+\eta\sin\mathbf{v}) \\
\quad +2(\varpi-1)^2\cos^2\mathbf{v} - (\varpi-1)^3\cos^3\mathbf{v}\Big) \\
\quad -3(\varpi-1)\cos^2\mathbf{v}\Big((\varpi-1)((\epsilon+1)\cos\mathbf{v}+\eta\sin\mathbf{v}) \\
\quad +2(\varpi-1)^2\cos^2\mathbf{v} - (\varpi-1)^3\cos^3\mathbf{v}\Big) \\
\quad -(\varpi-1)((\epsilon+1)\cos\mathbf{v}+\eta\sin\mathbf{v}) + 24(\varpi-1)^2(\cos^2\mathbf{v}-\sin^2\mathbf{v}) \\
\quad +3(\varpi-1)^3(20\cos\mathbf{v}\sin^2\mathbf{v} - 7\cos^3\mathbf{v}) + 2(\varpi-1)((\epsilon+1)\cos\mathbf{v}+\eta\sin\mathbf{v}) \\
\quad -6(\varpi-1)^3(\cos^3\mathbf{v} - 2\cos\mathbf{v}\sin^2\mathbf{v}) + \eta(\varpi-1)((\epsilon+1)\sin\mathbf{v}-\eta\cos\mathbf{v}) \\
\quad +16(\varpi-1)^2\cos\mathbf{v}\sin\mathbf{v} + 3(\varpi-1)^3(2\sin^3\mathbf{v} - 7\cos^2\mathbf{v}\sin\mathbf{v})
\end{cases} \\
&\quad +\dots , \\
\bar{\mathbf{U}}(\mathbf{v},\lambda,\varpi) \quad &= (1-\varpi)\cos\mathbf{v} + \frac{1}{\mathbf{N}(\delta)}\Big[(1-\varpi)\Big((\epsilon+1)\cos\mathbf{v}+\eta\sin\mathbf{v}\Big) + 2(1-\varpi)^2\cos^2\mathbf{v} \\
&\quad -(1-\varpi)^3\cos^3\mathbf{v}\Big] \\
&\quad \times\Big\{\frac{\delta\lambda^\delta}{\Gamma(\delta+1)} + (1-\delta)\Big\} \\
&\quad + \frac{1}{\mathbf{N}^2(\delta)}\Big\{\frac{\delta^2\lambda^{2\delta}}{\Gamma(2\delta+1)} + 2\delta(1-\delta)\frac{\lambda^\delta}{\Gamma(\delta+1)} + (1-\delta)^2\Big\} \\
&\quad \times\begin{cases}
\epsilon\Big((1-\varpi)((\epsilon+1)\cos\mathbf{v}+\eta\sin\mathbf{v}) + 2(1-\varpi)^2\cos^2\mathbf{v} - (1-\varpi)^3\cos^3\mathbf{v}\Big) \\
\quad +4(1-\varpi)\cos\mathbf{v}\Big((1-\varpi)((\epsilon+1)\cos\mathbf{v}+\eta\sin\mathbf{v}) + 2(1-\varpi)^2\cos^2\mathbf{v} \\
\quad -(1-\varpi)^3\cos^3\mathbf{v}\Big) - 3(1-\varpi)\cos^2\mathbf{v}\Big((1-\varpi)((\epsilon+1)\cos\mathbf{v}+\eta\sin\mathbf{v}) \\
\quad +2(1-\varpi)^2\cos^2\mathbf{v} - (1-\varpi)^3\cos^3\mathbf{v}\Big) - (1-\varpi)((\epsilon+1)\cos\mathbf{v}+\eta\sin\mathbf{v}) \\
\quad +24(1-\varpi)^2(\cos^2\mathbf{v}-\sin^2\mathbf{v}) + 3(1-\varpi)^3(20\cos\mathbf{v}\sin^2\mathbf{v} - 7\cos^3\mathbf{v}) \\
\quad +2(1-\varpi)((\epsilon+1)\cos\mathbf{v}+\eta\sin\mathbf{v}) - 6(1-\varpi)^3(\cos^3\mathbf{v} - 2\cos\mathbf{v}\sin^2\mathbf{v}) \\
\quad +\eta(1-\varpi)((\epsilon+1)\sin\mathbf{v}-\eta\cos\mathbf{v}) + 16(1-\varpi)^2\cos\mathbf{v}\sin\mathbf{v} \\
\quad +3(1-\varpi)^3(2\sin^3\mathbf{v} - 7\cos^2\mathbf{v}\sin\mathbf{v})
\end{cases} \\
&\quad +\dots .
\end{aligned} \tag{4.20}$$

Figure 7 shows the effects of the two (a) and various (b) 3D depictions for Example 4.4, as coupled with the ABCand Elzaki transform via the fuzzy system in this research. The discrepancy in $\tilde{\mathbf{U}}(\mathbf{v}, \lambda; \varpi)$ on the space coordinate $\mathbf{v}$ with respect to λ and the ambiguity component $\varpi \in [0, 1]$ is notably highlighted by the characteristic.

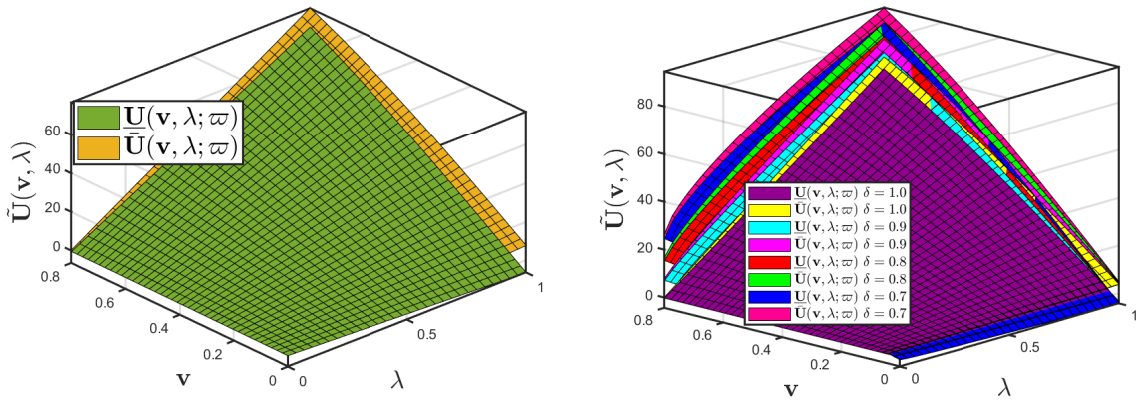

(a) **(b)**

Figure 7. (a) Fuzzy EADM-provided 3D-illustrations of Example 4.4 when $\delta = 1, \epsilon = 10$ and $\eta = 100$. (b) Fuzzy EADM-provided 3D-illustrations of multiple profiles of Example 4.4 when $\epsilon = 10, \eta = 100$ and $\varpi \in [0, 1]$.

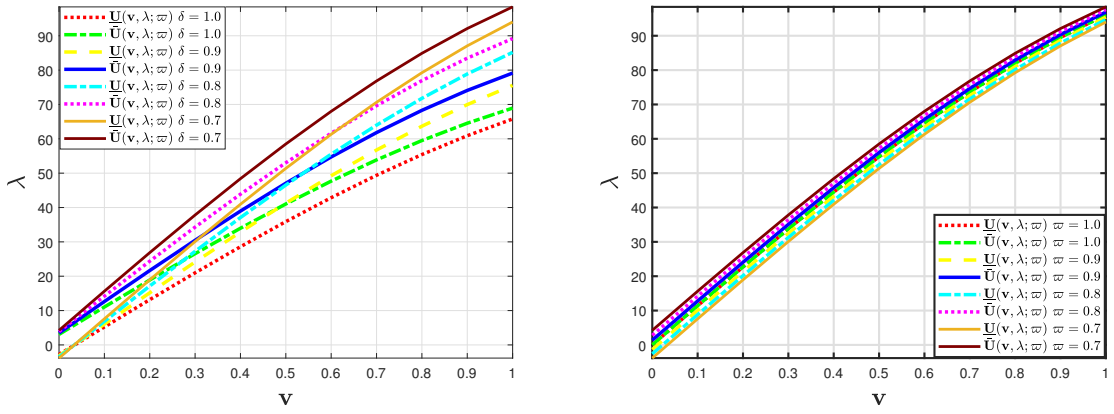

(a) **(b)**

Figure 8. (a) Fuzzy EADM-provided 2D-illustrations of multiple profiles of Example 4.4 when $\varpi = 0.7$, $\eta = \epsilon = 100$ and $\lambda = 0.5$; (b) Fuzzy EADM-provided 2D-illustrations of multiple profiles of Example 4.4 when $\delta = 0.7$ *and* $\lambda = 0.5$ with varying fractional order.

The research has shown that the graphical representation of $\tilde{\mathbf{U}}(\mathbf{v}, \lambda; \varpi)$ will progress to become increasingly complicated as time passes.

• Figure 8 exhibits the mapping accuracy of the recommended approach, $\tilde{\mathbf{U}}(\mathbf{v}, \lambda; \varpi)$, with the control variables $\eta = 100$ and $\epsilon = 10$. The research has revealed that the improvement in $\bar{\mathbf{U}}(\mathbf{v}, \lambda; \varpi)$ translates to a slight increase in $\underline{\mathbf{U}}(\mathbf{v}, \lambda; \varpi)$.

• In Figure 8, the ambiguity factors of the transformations $\underline{\mathbf{U}}(\mathbf{v},\lambda;\varpi)$ and $\bar{\mathbf{U}}(\mathbf{v},\lambda;\varpi)$ are depicted; the results show the performance of the prescribed fractional-order at multiple ambiguity factors.
• Figures 7 and 8 illustrate the aforementioned plots, which allow us to clarify the probabilistic nature of spatial and temporal fluctuations. Secondly, by employing an inferential probabilistic assessment, researchers involved in fields related to pattern generation, optical engineering, and probabilistic kinetics will be able to evaluate success. Finally, improved illustrations of the fluid dynamics robustness with bifurcated and scattering characteristics are conceivable.

Remark 4.4. If $\varpi-1=1-\varpi=1$ and $\delta=1$, then Eq (4.20) converges to the exact solution proposed in [39, 40].

Example 4.5. Suppose that the fuzzy fractional-order SHM is subject to fuzzy ICs

$$\begin{aligned}&\frac{\partial^{\delta}}{\partial\lambda^{\delta}}\tilde{\mathbf{U}}(\mathbf{v},\lambda;\varpi)=(\wp-1)\odot\tilde{\mathbf{U}}(\mathbf{v},\lambda;\varpi)\ominus\tilde{\mathbf{U}}^{3}(\mathbf{v},\lambda;\varpi)\ominus\frac{\partial^{4}}{\partial\mathbf{v}^{4}}\tilde{\mathbf{U}}(\mathbf{v},\lambda;\varpi)\ominus 2\odot\frac{\partial^{2}}{\partial\mathbf{v}^{2}}\tilde{\mathbf{U}}(\mathbf{v},\lambda;\varpi),\\&\tilde{\mathbf{U}}(\mathbf{v},0)=\tilde{\Upsilon}(\varpi)\odot\frac{1}{10}\sin\left(\frac{\pi\mathbf{v}}{\varrho}\right),\end{aligned}\tag{4.21}$$

where $\tilde{\Upsilon}(\varpi)=[\underline{\Upsilon}(\varpi),\bar{\Upsilon}(\varpi)]=[\varpi-1,1-\varpi]$ and there is a fuzzy number $\varpi\in[0,1]$.

The parametric form of Eq (4.21) is presented as:

$$\begin{cases}\frac{\partial^{\delta}}{\partial\lambda^{\delta}}\underline{\mathbf{U}}(\mathbf{v},\lambda;\varpi)=(\wp-1)\underline{\mathbf{U}}(\mathbf{v},\lambda;\varpi)-\underline{\mathbf{U}}^{3}(\mathbf{v},\lambda;\varpi)-\frac{\partial^{4}}{\partial\mathbf{v}^{4}}\underline{\mathbf{U}}(\mathbf{v},\lambda;\varpi)-2\frac{\partial^{2}}{\partial\mathbf{v}^{2}}\underline{\mathbf{U}}(\mathbf{v},\lambda;\varpi),\\ \underline{\mathbf{U}}(\mathbf{v},0)=(\underline{\Upsilon}(\varpi))\frac{1}{10}\sin\left(\frac{\pi\mathbf{v}}{\varrho}\right),\\ \frac{\partial^{\delta}}{\partial\lambda^{\delta}}\bar{\mathbf{U}}(\mathbf{v},\lambda;\varpi)=(\wp-1)\bar{\mathbf{U}}(\mathbf{v},\lambda;\varpi)-\bar{\mathbf{U}}^{3}(\mathbf{v},\lambda;\varpi)-\frac{\partial^{4}}{\partial\mathbf{v}^{4}}\bar{\mathbf{U}}(\mathbf{v},\lambda;\varpi)-2\frac{\partial^{2}}{\partial\mathbf{v}^{2}}\bar{\mathbf{U}}(\mathbf{v},\lambda;\varpi),\\ \bar{\mathbf{U}}(\mathbf{v},0)=\bar{\Upsilon}(\varpi)\frac{1}{10}\sin\left(\frac{\pi\mathbf{v}}{\varrho}\right).\end{cases}\tag{4.22}$$

Here, we examine the first instance of Eq (4.22) in an attempt to determine the EADM solution. In view of the procedure outlined in Section 3, we have

$$\begin{aligned}&\frac{\mathbf{N}(\delta)}{1-\delta+\delta\varphi^{\delta}}\mathbb{E}[\underline{\mathbf{U}}(\mathbf{v},\lambda;\varpi)]-\frac{\varphi^{2}\mathbf{N}(\delta)}{1-\delta+\delta\varphi^{\delta}}\underline{\mathbf{U}}_{(\kappa)}(\mathbf{v};\varpi)\\&=\mathbb{E}\left[(\wp-1)\underline{\mathbf{U}}(\mathbf{v},\lambda;\varpi)-\underline{\mathbf{U}}^{3}(\mathbf{v},\lambda;\varpi)-\frac{\partial^{4}}{\partial\mathbf{v}^{4}}\underline{\mathbf{U}}(\mathbf{v},\lambda;\varpi)-2\frac{\partial^{2}}{\partial\mathbf{v}^{2}}\underline{\mathbf{U}}(\mathbf{v},\lambda;\varpi)\right].\end{aligned}$$

Simple calculations show that

$$\begin{aligned}\underline{\mathbf{U}}(\mathbf{v},\lambda;\varpi)\quad&=(\varpi-1)\frac{1}{10}\sin\left(\frac{\pi\mathbf{v}}{\varphi}\right)\\&\quad+\mathbb{E}^{-1}\left[\frac{1-\delta+\delta\varphi^{\delta}}{\mathbf{N}(\delta)}\mathbb{E}\left[(\wp-1)\underline{\mathbf{U}}(\mathbf{v},\lambda;\varpi)-\underline{\mathbf{U}}^{3}(\mathbf{v},\lambda;\varpi)-\frac{\partial^{4}}{\partial\mathbf{v}^{4}}\underline{\mathbf{U}}(\mathbf{v},\lambda;\varpi)\right.\right.\\&\quad\left.\left.-2\frac{\partial^{2}}{\partial\mathbf{v}^{2}}\underline{\mathbf{U}}(\mathbf{v},\lambda;\varpi)\right]\right].\end{aligned}\tag{4.23}$$

We assume the infinite sum $\underline{\mathbf{U}}(\mathbf{v},\lambda;\varpi) = \sum_{q=0}^{\infty}\underline{\mathbf{U}}_q(\mathbf{v},\lambda;\varpi)$ incorporates Eq (3.5) and validate the non-linearity. As a result, Eq (4.23) leads to the formation

$$\begin{aligned}\sum_{q=0}^{\infty}\underline{\mathbf{U}}_q(\mathbf{v},\lambda;\varpi) &= (\varpi-1)\frac{1}{10}\sin\left(\frac{\pi\mathbf{v}}{\varrho}\right)+\mathbb{E}^{-1}\Bigg[\frac{1-\delta+\delta\varphi^{\delta}}{\mathbf{N}(\delta)}\\ &\times\mathbb{E}\Bigg[(\wp-1)\sum_{q=0}^{\infty}\underline{\mathbf{U}}_q(\mathbf{v},\lambda;\varpi)-\sum_{q=0}^{\infty}\underline{\mathbf{A}}_q(\mathbf{v},\lambda;\varpi)-\frac{\partial^4}{\partial\mathbf{v}^4}\sum_{q=0}^{\infty}\underline{\mathbf{U}}_q(\mathbf{v},\lambda;\varpi)\\ &-2\frac{\partial^2}{\partial\mathbf{v}^2}\sum_{q=0}^{\infty}\underline{\mathbf{U}}_q(\mathbf{v},\lambda;\varpi)\Bigg]\Bigg]. \end{aligned}\tag{4.24}$$

The foregoing formulae have two non-linear terms such as $\underline{\mathbf{U}}^3 = \sum_{q=0}^{\infty}\underline{\mathbf{A}}_q$ and $\underline{\mathbf{U}}^2 = \sum_{q=0}^{\infty}\underline{\mathbf{B}}_q$ which can be examined by using the Adomian polynomial defined by Eq (3.4); then, the Eq (4.24) diminishes to

$$\begin{aligned}\underline{\mathbf{U}_0}(\mathbf{v},\lambda;\varpi) &= (\varpi-1)\frac{1}{10}\sin\left(\frac{\pi\mathbf{v}}{\varrho}\right),\\ \underline{\mathbf{U}_1}(\mathbf{v},\lambda;\varpi) &= \mathbb{E}^{-1}\Bigg[\frac{1-\delta+\delta\varphi^{\delta}}{\mathbf{N}(\delta)}\mathbb{E}\Bigg[(\wp-1)\underline{\mathbf{U}}_0(\mathbf{v},\lambda;\varpi)-\frac{\partial^4}{\partial\mathbf{v}^4}\underline{\mathbf{U}}_0(\mathbf{v},\lambda;\varpi)-2\frac{\partial^2}{\partial\mathbf{v}^2}\underline{\mathbf{U}}_0(\mathbf{v},\lambda;\varpi)\\ &\quad-\underline{\mathbf{A}}_0(\mathbf{v},\lambda;\varpi)\Bigg]\Bigg]\\ &= \frac{1}{1000\varrho^4\mathbf{N}(\delta)}\Big[(\varpi-1)\sin\left(\frac{\pi\mathbf{v}}{\varrho}\right)\Big(100\varrho^4(\wp-1)-100\pi^4+200\pi^2\varrho^2\Big)\\ &\quad-\varrho^4(\varpi-1)^3\sin^3\left(\frac{\pi\mathbf{v}}{\varrho}\right)\Big]\Big\{\frac{\delta\lambda^{\delta}}{\Gamma(\delta+1)}+(1-\delta)\Big\},\\ \underline{\mathbf{U}_2}(\mathbf{v},\lambda;\varpi) &= \mathbb{E}^{-1}\Bigg[\frac{1-\delta+\delta\varphi^{\delta}}{\mathbf{N}(\delta)}\mathbb{E}\Bigg[(\wp-1)\underline{\mathbf{U}}_1(\mathbf{v},\lambda;\varpi)-\frac{\partial^4}{\partial\mathbf{v}^4}\underline{\mathbf{U}}_1(\mathbf{v},\lambda;\varpi)-2\frac{\partial^2}{\partial\mathbf{v}^2}\underline{\mathbf{U}}_1(\mathbf{v},\lambda;\varpi)\\ &\quad-\underline{\mathbf{A}}_1(\mathbf{v},\lambda;\varpi)\Bigg]\Bigg]\\ &= \frac{1}{\mathbf{N}^2(\delta)}\Big\{\frac{\delta^2\lambda^{2\delta}}{\Gamma(2\delta+1)}+2\delta(1-\delta)\frac{\lambda^{\delta}}{\Gamma(\delta+1)}+(1-\delta)^2\Big\}\\ &\quad\times\begin{Bmatrix}(100\varrho^4(\wp-1)-100\pi^4+2000\pi^2\varrho^2)\Big[\frac{(\wp-1)(\varpi-1)\pi}{1000\varrho^5}\cos\left(\frac{\pi\mathbf{v}}{\varrho}\right)\\ -\frac{\pi^4}{1000\varrho^8}(\varpi-1)\sin\left(\frac{\pi\mathbf{v}}{\varrho}\right)+\frac{2\pi^2}{1000\varrho^6}(\varpi-1)\sin\left(\frac{\pi\mathbf{v}}{\varrho}\right)\\ -\frac{3}{100000\varrho^4}(\varpi-1)^3\sin^4\left(\frac{\pi\mathbf{v}}{\varrho}\right)\Big]\\ -\sin^2\left(\frac{\pi\mathbf{v}}{\varrho}\right)\cos\left(\frac{\pi\mathbf{v}}{\varrho}\right)\Big(\frac{3\pi(\wp-1)}{1000\varrho}(\varpi-1)^3+\frac{42\pi^3}{1000\varrho^3}(\varpi-1)^3\Big)\\ -\frac{60\pi^4}{1000\varrho^4}(\varpi-1)^3\sin\left(\frac{\pi\mathbf{v}}{\varrho}\right)\cos^2\left(\frac{\pi\mathbf{v}}{\varrho}\right)+\frac{21\pi^4}{1000\varrho^4}(\varpi-1)^3 sin^3\left(\frac{\pi\mathbf{v}}{\varrho}\right)\\ +\frac{12\pi^3}{1000\varrho^3}(\varpi-1)^3\cos^3\left(\frac{\pi\mathbf{v}}{\varrho}\right)+\frac{3}{100000}(\varpi-1)^5\sin^6\left(\frac{\pi\mathbf{v}}{\varrho}\right)\end{Bmatrix},\\ &\vdots.\end{aligned}$$

In a similar way, additional elements of the EADM system $\underline{\mathbf{U}}q$ ($q \geq 3$) can be identified. Furthermore, as the iterative technique develops, the attained result's trustworthiness improves significantly and the established result appears progressively comparable to the expressive context. As a result, we have formulated a set of solutions that are structured in a series of formulations; that is,

$$\tilde{\mathbf{U}}(\mathbf{v},\lambda,\varpi) = \tilde{\mathbf{U}}_0(\mathbf{v},\lambda,\varpi) + \tilde{\mathbf{U}}_1(\mathbf{v},\lambda,\varpi) + \tilde{\mathbf{U}}_1(\mathbf{v},\lambda,\varpi) + ...$$

such that

$$\begin{aligned}
\underline{\mathbf{U}}(\mathbf{v},\lambda,\varpi) &= \underline{\mathbf{U}}_0(\mathbf{v},\lambda,\varpi) + \underline{\mathbf{U}}_1(\mathbf{v},\lambda,\varpi) + \underline{\mathbf{U}}_1(\mathbf{v},\lambda,\varpi) + ... ,\\
\bar{\mathbf{U}}(\mathbf{v},\lambda,\varpi) &= \bar{\mathbf{U}}_0(\mathbf{v},\lambda,\varpi) + \bar{\mathbf{U}}_1(\mathbf{v},\lambda,\varpi) + \bar{\mathbf{U}}_1(\mathbf{v},\lambda,\varpi) + ...
\end{aligned}$$

Eventually, we have

$$\begin{aligned}
\underline{\mathbf{U}}(\mathbf{v},\lambda,\varpi) &= (\varpi-1)\frac{1}{10}\sin\left(\frac{\pi\mathbf{v}}{\varrho}\right)\\
&\quad+\frac{1}{1000\varrho^4\mathbf{N}(\delta)}\Big[(\varpi-1)\sin\left(\frac{\pi\mathbf{v}}{\varrho}\right)\Big(100\varrho^4(\wp-1)-100\pi^4+200\pi^2\varrho^2\Big)\\
&\quad-\varrho^4(\varpi-1)^3\sin^3\left(\frac{\pi\mathbf{v}}{\varrho}\right)\Big]\Big\{\frac{\delta\lambda^\delta}{\Gamma(\delta+1)}+(1-\delta)\Big\}\\
&\quad+\frac{1}{\mathbf{N}^2(\delta)}\Big\{\frac{\delta^2\lambda^{2\delta}}{\Gamma(2\delta+1)}+2\delta(1-\delta)\frac{\lambda^\delta}{\Gamma(\delta+1)}+(1-\delta)^2\Big\}\\
&\quad\times\begin{cases}
(100\varrho^4(\wp-1)-100\pi^4+2000\pi^2\varrho^2)\Big[\frac{(\wp-1)(\varpi-1)\pi}{1000\varrho^5}\cos\left(\frac{\pi\mathbf{v}}{\varrho}\right)\\
\quad-\frac{\pi^4}{1000\varrho^8}(\varpi-1)\sin\left(\frac{\pi\mathbf{v}}{\varrho}\right)+\frac{2\pi^2}{1000\varrho^6}(\varpi-1)\sin\left(\frac{\pi\mathbf{v}}{\varrho}\right)\\
\quad-\frac{3}{100000\varrho^4}(\varpi-1)^3\sin^4\left(\frac{\pi\mathbf{v}}{\varrho}\right)\Big]\\
\quad-\sin^2\left(\frac{\pi\mathbf{v}}{\varrho}\right)\cos\left(\frac{\pi\mathbf{v}}{\varrho}\right)\Big(\frac{3\pi(\wp-1)}{1000\varrho}(\varpi-1)^3+\frac{42\pi^3}{1000\varrho^3}(\varpi-1)^3\Big)\\
\quad-\frac{60\pi^4}{1000\varrho^4}(\varpi-1)^3\sin\left(\frac{\pi\mathbf{v}}{\varrho}\right)\cos^2\left(\frac{\pi\mathbf{v}}{\varrho}\right)+\frac{21\pi^4}{1000\varrho^4}(\varpi-1)^3 sin^3\left(\frac{\pi\mathbf{v}}{\varrho}\right)\\
\quad+\frac{12\pi^3}{1000\varrho^3}(\varpi-1)^3\cos^3\left(\frac{\pi\mathbf{v}}{\varrho}\right)+\frac{3}{100000}(\varpi-1)^5\sin^6\left(\frac{\pi\mathbf{v}}{\varrho}\right)
\end{cases}\\
&\quad+... ,\\
\bar{\mathbf{U}}(\mathbf{v},\lambda,\varpi) &= (1-\varpi)\frac{1}{10}\sin\left(\frac{\pi\mathbf{v}}{\varrho}\right)\\
&\quad+\frac{1}{1000\varrho^4\mathbf{N}(\delta)}\Big[(1-\varpi)\sin\left(\frac{\pi\mathbf{v}}{\varrho}\right)\Big(100\varrho^4(\wp-1)-100\pi^4+200\pi^2\varrho^2\Big)\\
&\quad-\varrho^4(1-\varpi)^3\sin^3\left(\frac{\pi\mathbf{v}}{\varrho}\right)\Big]\Big\{\frac{\delta\lambda^\delta}{\Gamma(\delta+1)}+(1-\delta)\Big\}\\
&\quad+\frac{1}{\mathbf{N}^2(\delta)}\Big\{\frac{\delta^2\lambda^{2\delta}}{\Gamma(2\delta+1)}+2\delta(1-\delta)\frac{\lambda^\delta}{\Gamma(\delta+1)}+(1-\delta)^2\Big\}
\end{aligned}$$

$$\times\begin{Bmatrix}(100\varrho^4(\wp-1)-100\pi^4+2000\pi^2\varrho^2)\Big[\frac{(\wp-1)(1-\varpi)\pi}{1000\varrho^5}\cos\big(\frac{\pi\mathbf{v}}{\varrho}\big)\\ -\frac{\pi^4}{1000\varrho^8}(1-\varpi)\sin\big(\frac{\pi\mathbf{v}}{\varrho}\big)+\frac{2\pi^2}{1000\varrho^6}(1-\varpi)\sin\big(\frac{\pi\mathbf{v}}{\varrho}\big)\\ -\frac{3}{100000\varrho^4}(1-\varpi)^3\sin^4\big(\frac{\pi\mathbf{v}}{\varrho}\big)\Big]\\ -\sin^2\big(\frac{\pi\mathbf{v}}{\varrho}\big)\cos\big(\frac{\pi\mathbf{v}}{\varrho}\big)\Big(\frac{3\pi(\wp-1)}{1000\varrho}(1-\varpi)^3+\frac{42\pi^3}{1000\varrho^3}(1-\varpi)^3\Big)\\ -\frac{60\pi^4}{1000\varrho^4}(1-\varpi)^3\sin\big(\frac{\pi\mathbf{v}}{\varrho}\big)\cos^2\big(\frac{\pi\mathbf{v}}{\varrho}\big)+\frac{21\pi^4}{1000\varrho^4}(1-\varpi)^3 sin^3\big(\frac{\pi\mathbf{v}}{\varrho}\big)\\ +\frac{12\pi^3}{1000\varrho^3}(1-\varpi)^3\cos^3\big(\frac{\pi\mathbf{v}}{\varrho}\big)+\frac{3}{100000}(1-\varpi)^5\sin^6\big(\frac{\pi\mathbf{v}}{\varrho}\big)\end{Bmatrix}$$
$$+\ldots\ .$$

(4.25)

Figure 9 demonstrates the implications of two (a) and numerous (b) 3D depictions for Example 4.5, which correspond with the ABCand Elzaki transform via the fuzzy system in this research. The deviations in $\tilde{\mathbf{U}}(\mathbf{v},\lambda;\varpi)$ on the space coordinate $\mathbf{v}$ with respect to λ and the ambiguity component $\varpi\in[0,1]$ are delightfully exhibited by the analysis.

The investigation has revealed that the depiction of $\tilde{\mathbf{U}}(\mathbf{v},\lambda;\varpi)$ will develop extremely complicated as time passes.

• Figure 10 displays the mapping capability of the proposed technique, $\tilde{\mathbf{U}}(\mathbf{v},\lambda;\varpi)$, with the control variables $\wp=5$ and $\varrho=5$. The study indicates that the reduction in $\bar{\mathbf{U}}(\mathbf{v},\lambda;\varpi)$ results in a slight boost in $\underline{\mathbf{U}}(\mathbf{v},\lambda;\varpi)$.

• In Figure 10, the ambiguity components of the mappings $\underline{\mathbf{U}}(\mathbf{v},\lambda;\varpi)$ and $\bar{\mathbf{U}}(\mathbf{v},\lambda;\varpi)$ are represented; the results demonstrate the action of the prescribed fuzzy fractional-order of the mapping for distinct ambiguity factors.

• Figures 9 and 10 depict the preceding plots, which allow us to understand the probabilistic patterns of spatial and temporal variability. In addition, the inferential statistical analysis of the proposed method will assist researchers engaged in research on pattern generation, optical engineering and probabilistic kinetics in analyzing efficacy. As a consequence, as the repetitive procedure is intensified, superior estimations can be developed.

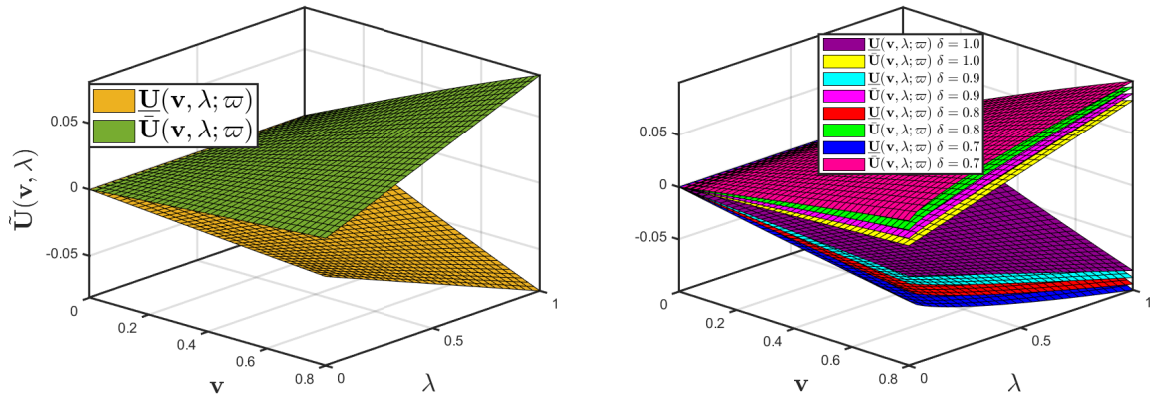

(a) **(b)**

Figure 9. (a) Fuzzy EADM-provided 3D-illustrations of Example 4.5 when $\delta=1,\wp=5$ and $\varrho=100$. (b) Fuzzy EADM-provided 3D-illustrations of multiple profiles of Example 4.5 when $\wp=10,\varrho=100$ and $\varpi\in[0,1]$.

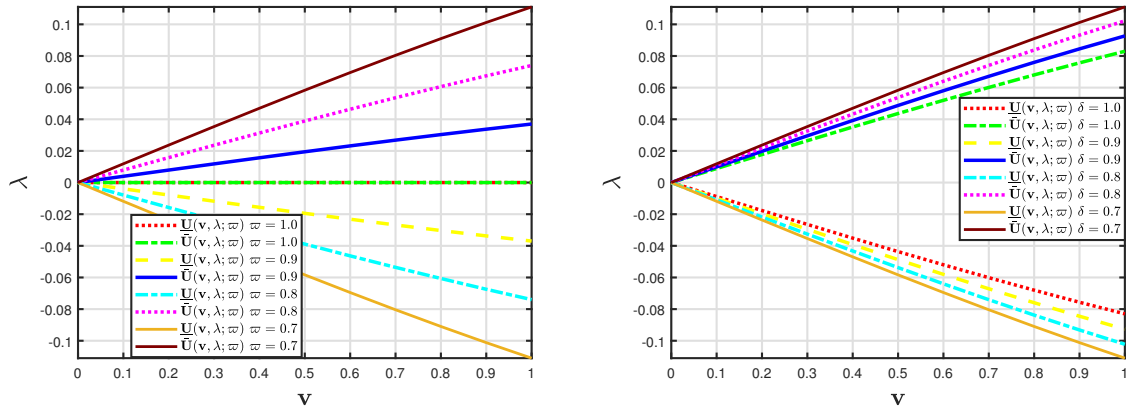

(a) **(b)**

Figure 10. (a) Fuzzy EADM-provided 2D-illustrations of multiple profiles of Example 4.3 when $\varpi = 0.7$, $\varrho = 0.8$, $\wp = 0.5$ and $\lambda = 0.5$; (b) Fuzzy EADM-provided 2D-illustrations of multiple profiles of Example 4.3 when $\delta = 0.7$ *and* $\lambda = 0.9$ with varying fractional-order.

Remark 4.5. If $\varpi - 1 = 1 - \varpi = 1$ and $\delta = 1$, then Eq (4.25) converges to the exact solution proposed in [39, 40].

5. Conclusions

The SHM is concerned with pattern formation, it is considered a nonlinear PDE. This connection involves noise in bifurcations, pattern determination, spacetime chaos and imperfection mechanisms, all of which were explored in this study. The succinct formulation, on the other hand, is incapable of conveying any complex mechanism in an unknown setting. In this scenario, ambiguous variables provide an effective direction to depict the analytical method. We employed a fuzzy technique to investigate the SHM, compensating for IC unpredictability. In this study, we extended the fractional SHM to the fuzzy fractional SHM in the ABC framework. We next implemented the EADM to generate an estimated description of the projected scheme in its generic version. We developed a generic approach for every instance after considering various instances to verify the proposed technique. The numerical simulation results for 2D and 3D representations featuring different fractional-order and ambiguity factors were also analyzed. Because the consequence patterns fulfill the fuzzified constraints, we can see that they reflect the imprecise repercussions in the representations. The stability and inaccuracy of the offered technique have been examined. By relying on computations, we demonstrated that the fractional-order system shapes reflect integer-order solution trajectories. Consequently, the incorrect reasoning allows a system to function effectively in a fuzzy context. We shall explore an analogous topic in future research by introducing the Henstock integrals (i.e., fuzzy integrals in the Lebesgue sense) at infinite spacing [59, 60].

Conflict of interest

The authors declare that they have no competing interests.

References

1. I. Podlubny, *Fractional differential equations*, Lightning Source Inc, 1998.
2. K. Karthikeyan, P. Karthikeyan, H. M. Baskonus, K. Venkatachalam, Y. M. Chu, Almost sectorial operators on Ψ-Hilfer derivative fractional impulsive integro-differential equations, *Math. Method. Appl. Sci.*, 2021, https://doi.org/10.1002/mma.7954
3. H. Zhang, J. Cheng, H. Zhang, J. Cao, Quasi-uniform synchronization of Caputo type fractional neural networks with leakage and discrete delays, *Chaos Soliton. Fract.*, **152** (2021), 111432. https://doi.org/10.1016/j.chaos.2021.111432
4. C. Wang, H. Zhang, H. Zhang, W. Zhang, Globally projective synchronization for Caputo fractional quaternion-valued neural networks with discrete and distributed delays, *AIMS Math.*, **6** (2021), 14000–14012. https://doi.org/10.3934/math.2021809
5. F. Jin, Z. S. Qian, Y. M. Chu, M. ur Rahman, On nonlinear evolution model for drinking behavior under Caputo-Fabrizio derivative, *J. Appl. Anal. Comput.*, **12** (2022), 790–806. https://doi.org/10.11948/20210357
6. H. Zhang, Y. Cheng, H. Zhang, W. Zhang, J. Caocd, Hybrid control design for Mittag-Leffler projective synchronization on FOQVNNs with multiple mixed delays and impulsive effects, *Math. Comput. Simulat.*, **197** (2022), 341–357. https://doi.org/10.1016/j.matcom.2022.02.022
7. S. Rashid, S. Sultana, Y. Karaca, A. Khalid, Y. M. Chu, Some further extensions considering discrete proportional fractional operators, *Fractals*, **30** (2022), 2240026. https://doi.org/10.1142/S0218348X22400266
8. S. Narges Hajiseyedazizi, M. E. Samei, J. Alzabut, Y. M. Chu, On multi-step methods for singular fractional q-integro-differential equations, *Open Math.*, **19** (2021), 1378–1405. https://doi.org/10.1515/math-2021-0093
9. Y. Cheng, H. Zhang, W. Zhang, H. Zhang, Novel algebraic criteria on global Mittag-Leffler synchronization of FOINNs with the Caputo derivative and delay, *J. Appl. Math. Comput.*, 2021. https://doi.org/10.1007/s12190-021-01672-0
10. A. Atangana, D. Baleanu, New fractional derivatives with nonlocal and nonsingular kernel, theory and application to heat transfer model, *Therm. Sci.*, **20** (2016), 763–769. https://doi.org/10.2298/TSCI160111018A
11. S. Rashid, E. I. Abouelmagd, A. Khalid, F. B. Farooq, Y. M. Chu, Some recent developments on dynamical $\hbar$-discrete fractional type inequalities in the frame of nonsingular and nonlocal kernels, *Fractals*, **30** (2022), 2240110. https://doi.org/10.1142/S0218348X22401107
12. F. Z. Wang, M. N. Khan, I. Ahmad, H. Ahmad, H. Abu-Zinadah, Y. M. Chu, Numerical solution of traveling waves in chemical kinetics: Time-fractional fishers equations, *Fractals*, **30** (2022), 2240051. https://doi.org/10.1142/S0218348X22400515
13. S. Rashid, E. I. Abouelmagd, S. Sultana, Y. M. Chu, New developments in weighted n-fold type inequalities via discrete generalized $\hat{\text{h}}$-proportional fractional operators, *Fractals*, **30** (2022), 2240056. https://doi.org/10.1142/S0218348X22400564

14. S. A. Iqbal, M. G. Hafez, Y. M. Chu, C. Park, Dynamical Analysis of nonautonomous RLC circuit with the absence and presence of Atangana-Baleanu fractional derivative, *J. Appl. Anal. Comput.*, **12** (2022), 770–789. https://doi.org/10.11948/20210324

15. D. Kumar, J. Singh, D. Baleanu, Analysis of regularized long-wave equation associated with a new fractional operator with Mittag-leffler type kernel, *Physica A*, **492** (2018), 155–167. https://doi.org/10.1016/j.physa.2017.10.002

16. D. Kumar, J. Singh, K. Tanwar, D. Baleanu, A new fractional exothermic reactions model having constant heat source in porous media with power, exponential and mittag-leffler laws, *Int. J. Heat. Mass. Tran.*, **138** (2019), 1222–1227. https://doi.org/10.1016/j.ijheatmasstransfer.2019.04.094

17. S. Rashid, S. Sultana, Z. Hammouch, F. Jarad, Y. S. Hamed, Novel aspects of discrete dynamical type inequalities within fractional operators having generalized h-discrete Mittag-Leffler kernels and application, *Chaos Soliton. Fract.*, **151** (2021), 111204. https://doi.org/10.1016/j.chaos.2021.111204

18. W. M. Qian, H. H. Chu, M. K. Wang, Y. M. Chu, Sharp inequalities for the Toader mean of order -1 in terms of other bivariate means, *J. Math. Inequal.*, **16** (2022), 127–141. https://doi.org/10.7153/jmi-2022-16-10

19. T. H. Zhao, H. H. Chu, Y. M. Chu, Optimal Lehmer mean bounds for the *n*th power-type Toader mean of $n = -1, 1, 3$, *J. Math. Inequal.*, **16** (2022), 157–168. https://doi.org/10.7153/jmi-2022-16-12

20. M. Toufik, A. Atangana, New numerical approximation of fractional derivative with non-local and non-singular kernel: Application to chaotic models, *Eur. Phys. J. Plus*, **132** (2017), 144. https://doi.org/10.1140/epjp/i2017-11717-0

21. M. Nazeer, F. Hussain, M. Ijaz Khan, Asad-ur-Rehman, E. R. El-Zahar, Y. M. Chu, et al., Theoretical study of MHD electro-osmotically flow of third-grade fluid in micro channel, *Appl. Math. Comput.*, **420** (2022), 126868. https://doi.org/10.1016/j.amc.2021.126868

22. Y. M. Chu, B. M. Shankaralingappa, B. J. Gireesha, F. Alzahrani, M. Ijaz Khan, S. U. Khan, Combined impact of Cattaneo-Christov double diffusion and radiative heat flux on bio-convective flow of Maxwell liquid configured by a stretched nano-material surface, *Appl. Math. Comput.*, **419** (2022), 126883. https://doi.org/10.1016/j.amc.2021.126883

23. T. H. Zhao, M. Ijaz Khan, Y. M. Chu, Artificial neural networking (ANN) analysis for heat and entropy generation in flow of non-Newtonian fluid between two rotating disks, *Math. Method. Appl. Sci.*, 2021. https://doi.org/10.1002/mma.7310

24. Y. M. Chu, U. Nazir, M. Sohail, M. M. Selim, J. R. Lee, Enhancement in thermal energy and solute particles using hybrid nanoparticles by engaging activation energy and chemical reaction over a parabolic surface via finite element approach, *Fractal Fract.*, **5** (2021), 119. https://doi.org/10.3390/fractalfract5030119

25. N. V. Hoa, H. Vu, T. M. Duc, Fuzzy fractional differential equations under Caputo Katugampola fractional derivative approach, *Fuzzy Set. Syst.*, **375** (2019), 70–99. https://doi.org/10.1016/j.fss.2018.08.001

26. N. V. Hoa, Fuzzy fractional functional differential equations under Caputo gH-differentiability, *Commun. Nonlinear Sci.*, **22** (2015), 1134–1157. https://doi.org/10.1016/j.cnsns.2014.08.006

27. S. L. Chang, L. A. Zadeh, On fuzzy mapping and control, *IEEE T. Syst. Man Cy.*, **2** (1972), 30–34. https://doi.org/10.1142/9789814261302_0012

28. D. Dubois, H. Prade, Towards fuzzy differential calculus part 3: Differentiation, *Fuzzy Set. Syst.*, **8** (1982), 225–233. https://doi.org/10.1016/S0165-0114(82)80001-8

29. K. M. Saad, A reliable analytical algorithm for spacetime fractional cubic isothermal autocatalytic chemical system, *Pramana*, **91** (2018), 51. https://doi.org/10.1007/s12043-018-1620-3

30. K. M. Saad, J. F. Gómez-Aguilar, Analysis of reactiondiffusion system via a new fractional derivative with non-singular kernel, *Physica A*, **509** (2018), 703–7116. https://doi.org/10.1016/j.physa.2018.05.137

31. O. A. Arqub, M. Al-Smadi, S. Momani, T. Hayat, Application of reproducing kernel algorithm for solving second-order, two-point fuzzy boundary value problems, *Soft Comput.*, **21** (2017), 7191–7206. https://doi.org/10.1007/s00500-016-2262-3

32. O. A. Arqub, Adaptation of reproducing kernel algorithm for solving fuzzy Fredholm-Volterra integrodifferential equations, *Neural Comput. Appl.*, **28** (2017), 15911610. https://doi.org/10.1007/s00521-015-2110-x

33. S. Rashid, F. Jarad, K. M. Abualnaja, On fuzzy Volterra-Fredholm integrodifferential equation associated with Hilfer-generalized proportional fractional derivative, *AIMS Math.*, **6** (2021), 10920–10946. https://doi.org/10.3934/math.2021635

34. A. Kandel, W. J. Byatt, Fuzzy differential equations, In: *Proceedings of international conference cybernetics and society*, 1978, 1213–1216.

35. R. P. Agarwal, V. Lakshmikantham, J. J. Nieto, On the concept of solution for fractional differential equations with uncertainty, *Nonlinear Anal. Theor.*, **72** (2010), 2859–2862. https://doi.org/10.1016/j.na.2009.11.029

36. T. Allahviranloo, A. M. Kermani, Numerical methods for fuzzy partial differential equations under new defini-tion for derivative, *Iran. J. Fuzzy Syst.*, **7** (2010), 33–50.

37. O. A. Arqub, M. Al-Smadi, S. Momani, T. Hayat, Application of reproducing kernel algorithm for solving second-order, two-point fuzzy boundary value problems, *Soft Comput.*, **21** (2017), 7191–7206. https://doi.org/10.1007/s00500-016-2262-3

38. T. H. Zhao, O. Castillo, H. Jahanshahi, A. Yusuf, M. O. Alassafi, F. E. Alsaadi, et al., A fuzzy-based strategy to suppress the novel coronavirus (2019-NCOV) massive outbreak, *Appl. Comput. Math.*, **20** (2021), 160–176.

39. J. B. Swift, P. C. Hohenberg, Hydrodynamic fuctuations at the convective instability, *Phys. Rev. A*, **15** (1977), 319. https://doi.org/10.1103/PhysRevA.15.319

40. P. Hohenberg, J. B. Swift, Effects of additive noise at the onset of Rayleigh-Benard convection, *Phys. Rev. A*, **46** (1992), 4773–4785. https://doi.org/10.1103/PhysRevA.46.4773

41. L. Lega, J. V. Moloney, A. C. Newell, Swift-Hohenberg equation for lasers, *Phys. Rev. Lett.*, **73** (1994), 2978–2981. https://doi.org/10.1103/PhysRevLett.73.2978

42. M. C. Cross, P. C. Hohenberg, Pattern formulation outside of equiblirium, *Rev. Mod. Phys.*, **65** (1993), 851–1112. https://doi.org/10.1103/RevModPhys.65.851

43. W. Li, Y. Pang, An iterative method for time-fractional Swift-Hohenberg equation, *Adv. Math. Phys.*, **2018** (2018), 2405432. https://doi.org/10.1155/2018/2405432
44. N. A. Khan, N. U. Khan, M. Ayaz, A. Mahmood, Analytical methods for solving the time-fractional Swif-Hohenberg equation, *Comput. Math. Appl.*, **61** (2011), 2182–2185. https://doi.org/10.1016/j.camwa.2010.09.009
45. K. Vishal, S. Kumar, S. Das, Application of homotopy analysis method for fractional Swif Hohenberg equation-revisited, *Appl. Math. Model.*, **36** (2012), 3630–3637. https://doi.org/10.1016/j.apm.2011.10.001
46. K. Vishal, S. Das, S. H. Ong, P. Ghosh, On the solutions of fractional Swif Hohenberg equation with dispersion, *Appl. Math. Comput.*, **219** (2013), 5792–5801. https://doi.org/10.1016/j.amc.2012.12.032
47. M. Merdan, A numeric-analytic method for time-fractional Swif-Hohenberg equation with modifed Riemann-Liouville derivative, *Appl. Math. Model.*, **37** (2013), 4224–4231. https://doi.org/10.1016/j.apm.2012.09.003
48. S. Das, K. Vishal, Homotopy analysis method for fractional Swift-Hohenberg equation, In: *Advances in the homotopy analysis method*, 2014, 291–308. https://doi.org/10.1142/9789814551250_0007
49. T. M. Elzaki, The new integral transform Elzaki transform, *Global J. Pure Appl. Math.*, **7** (2011), 57–64.
50. G. Adomian, A review of the decomposition method in applied mathematics, *J. Math. Anal. Appl.*, **135** (1988), 501–544. https://doi.org/10.1016/0022-247X(88)90170-9
51. S. Rashid, R. Ashraf, E. Bonyah, On analytical solution of time-fractional biological population model by means of generalized integral transform with their uniqueness and convergence analysis, *Adv. Nonlinear Anal. Appl.*, **2022** (2022), 7021288. https://doi.org/10.1155/2022/7021288
52. S. Rashid, R. Ashraf, F. S. Bayones, A novel treatment of fuzzy fractional Swift-Hohenberg equation for a hybrid transform within the fractional derivative operator, *Fractal Fract.*, **5** (2021), 209. https://doi.org/10.3390/fractalfract5040209
53. T. Allahviranloo, *Fuzzy fractional differential operators and equations: Fuzzy fractional differential equations*, Springer Nature, 2021.
54. H. J. Zimmermann, *Fuzzy set theory and its applications*, Dordrecht: Kluwer Academic Publishers, 1991.
55. L. A. Zadeh, Fuzzy sets, *Inf. Control*, **8** (1965), 338–353.
56. S. Salahshour, A. Ahmadian, N. Senu, D. Baleanu, P. Agarwal, On analytical aolutions of the fractional differential equation with uncertainty: Application to the Basset problem, *Entropy*, **7** (2015), 885–902. https://doi.org/10.3390/e17020885
57. T. Allahviranloo, M. B. Ahmadi, Fuzzy lapalce transform, *Soft Comput.*, **14** (2010), 235–243. https://doi.org/10.1007/s00500-008-0397-6
58. M. Yavuz, T. Abdeljawad, Nonlinear regularized long-wave models with a new integral transformation applied to the fractional derivative with power and Mittag-Leffler kernel, *Adv. Differ. Equ.*, **2020** (2020), 367. https://doi.org/10.1186/s13662-020-02828-1

59. R. Henstock, *Theory of integration*, Butterworths, 1963.

60. Z. T. Gong, L. L. Wang, The Henstock-Stieltjes integral for fuzzy-number-valued functions, *Inform. Sciences*, **188** (2012), 276–297. https://doi.org/10.1016/j.ins.2011.11.024

AIMS Press